TWO – DIMENSIONAL ELECTRICAL IMAGING OF THE SUBSURFACE STRUCTURE OF BOMO DAM, ZARIA, NIGERIA

BY

OJO OLUFEMI FELIX
MSC/SCI/41975/04 – 05

A THESIS SUBMITTED TO THE POSTGRADUATE SCHOOL, AHMADU BELLO UNIVERSITY, ZARIA IN PARTIAL FULFILMENT OF THE REQUIREMENTS FOR THE AWARD OF THE DEGREE OF MASTER OF SCIENCE IN APPLIED GEOPHYSICS

DEPARTMENT OF PHYSICS
FACULTY OF SCIENCE
AHMADU BELLO UNIVERSITY, ZARIA

DECEMBER, 2007

DEDICATION

I dedicate this thesis to the Almighty God whose grace was sufficient for me throughout the period of my study.

DECLARATION

I declare that the work in the thesis entitled "Two - Dimensional Electrical Imaging of the Subsurface Structure of Bomo Dam" has been performed by me in the Department of Physics under the Supervision of Prof. I. B. Osazuwa and Dr. A. L. Ahmed. The information derived from the literature has been duly acknowledged in the text and a list of references provided. No part of this thesis was previously presented for another degree or diploma at any University.

_____

Ojo Olufemi Felix

_____ _____

Signature Date

CERTIFICATION

This thesis titled 2 D electrical imaging of the subsurface structure of Bomo Dam, Zaria, Nigeria by Ojo Olufemi Felix meets the regulation governing the award of degree of Master of Science in Applied Geophysics of Ahmadu Bello University and is approved for its contribution to knowledge and literary presentation.

_____ Date: _____

Prof. I. B. Osazuwa
Chairman Supervisory Committee

_____ Date: _____

Dr. A. L. Ahmed
Member, Supervisory Committee

_____ Date: _____

Prof. N. Hariharan
Head of Department

_____ Date: _____

Prof. S. A. Nkom
Dean Post Graduate School

ACKNOWLEDGMENT

First and foremost, I am very grateful to the Almighty God for his grace, mercy and divine protection throughout the period of my study.

My special thank goes to my amiable supervisor Prof. I. B. Osazuwa for his financial and fatherly support. Not only did he make available the equipments for the data collection, he also provided every material needed for the Processing of the data. Indeed, he gave me the opportunity to gain out of his immense knowledge. Sir, I am very grateful, I cannot thank you enough.

My special thank also goes to Dr. A. L. Ahmed for taking time to go through my work and his contribution to the success of the work

I cannot but appreciate with great thanks the encouragement and moral support of Engr. C. A. Bangbelu.

I owe my unreserved gratitude to Prof. S. B. Ojo, Prof. M. N. Umego, Dr. Peter Sule and Dr. Kola Lawal for giving me the opportunity to gain out of their immense knowledge.

I wish to acknowledge my senior colleagues most especially Chiemeke Collins, Gabriel, D. Chinadu, Ibe and S. O. Adetola for

their various contributions. I equally acknowledge the individual efforts of my colleagues, some of whom are Laide Kalejaye, Suny Inichinbia, El-khalil and Joseph Osumeje. I say thank you for your moral support.

I am particularly grateful to my parents Mr. and Mrs Ojo for their prayers and moral support. It would have been impossible for me to think of running a post graduate programme if I did not receive their support.

I cannot but extend my sincere appreciation to my wife, Motunrayo Ojo who stood solidly behind me in the time of needs. I am very grateful for your kind gesture.

I equally thank Miss Florence A. Ekele, Mr. Moshud, Mr. Oladiran, Mrs Babatunde, Mr. Douglas, Matthew Ojeka and Mr. Olakitan for their moral support and encouragement.

My Thanks also to the International Programme in the Physical Sciences (IPPS) of Uppsala University Sweden, for the facilities provided to the Geophysics group of this Department, which made the completion of this work possible, and also for the grants made available to me for the final production of this thesis.

ABSTRACT

2D electrical resistivity imaging was used to investigate the subsurface structure of Bomo dam in Zaria, Kaduna state. The dam was constructed by the institute of Agriculture Research, Ahmadu Bello University, Zaria for irrigation purpose. The major characteristics of the dam is that it is seasonal, it cannot hold its water throughout the year. The geophysical survey was conducted to determine the depth to the basement, the nature of the fracture system and the texture of the strata underlying the dam.

A total number of five profiles were taken along the boundaries of the Dam. The layout geometry for the electrical imaging was such that two reels of cables were used with 5m intervals between the electrodes. A total number of 42 electrodes were used. However, the two innermost electrodes adjoining the two reels of cables coincided thus yielding a total of 41electrodes and a spread length of 200m. The data obtained using ABEM Terrameter SAS 4000 were processed using RES2DIVN software.

The resistivity inversion results for the profiles show that the near surface material is not consolidated and that the weathered basement is highly fractured. From these results, it can be concluded that the seasonality of the dam is partly due to both the fracturing of the basement and the unconsolidated nature of the overburden.

TABLE OF CONTENTS

Title **Page**

Title Page i

Dedication..... ii

Declaration.....iii

Certification..... iv

Acknowledgement..... v

Abstract..... vi

Table of contents vii

List of Figures.....viii

List of Table.....xiii

CHAPTER ONE: INTRODUCTION

1.1 General 1

1.2 Climate and Geomorphology of Study Area 3

1.3 General Geology of the Study Area..... 6

1.3.1 The Older Metasediments 9

1.3.2 The Younger Metasediments 9

1.3.3 The Older Granite 10

1.3.4 The younger Granite.....10

1.4 Basement Geology around the Study Area 11

1.5 General Hydrogeology 12

1.6 Review of Previous Study ……12

1.7 Aim and Scope of Study ……14

CHAPTER TWO; PRINCIPLES AND THEORIES OF ELECTRICAL RESISTIVITY METHOD

2.1 Introduction ……...15

2.2 Electrical Resistivity Method …….....16

2.2.1 Vertical Electrical Sounding (VES)……18

2.2.2 Constant Separation Traversing (CST)……19

2.3 Factors Affecting Electrical Resistivity ……20

2.3.1 Water Salinity……..20

2.3.2 Porosity of Rock .....……21

2.3.3 Effect of Temperature ……..22

2.3.4 Effect of Rock Texture and Porosity ……....22

2.3.5 Effect of Geological Processes…….....23

2.3.6 Effect of Rock Type……23

2.4 Theory of the DC Resistivity Method……25

2.5 Concept of Apparent Resistivity……29

2.6 Limitations of Electrical Resistivity Method…….....30

CHAPTER THREE: FIELD SURVEY METHOD AND INSTRUMENTATION

3.1 Introduction……31

3.2 Electrode Arrays……36

3.2.1 Wenner Array……36

3.2.2 Dipole – dipole Array..……38

3.2.3 Wenner – Schlumberger Array..……..39

3.2.4 Pole – pole Array……..40

3.2.5 Pole – dipole ……..…..41

3.3 The Measurement Procedure for Wenner Electron Configuration…42

CHAPTER FOUR: INTERPRETATION AND RESULTS

4.1 Introduction……46

4.2 Interpretation Technique……...46

4.3 Geological Control…….50

4.4 The Inversion Method ……50

4.5 The Production of Pseudosection……52

4.6 Electrical Images along the Profiles……...54

4.6.1 Profile One ……54

4.6.2 Profile Two ……56

4.6.3 Profile Three ……..58

4.6.4 Profile Four ……60

4.6.5 Profile Five ……62

CHAPTER FIVE: DISCUSSION, CONCLUSION AND RECOMMENDATIONS

5.1 Conclusion …….....64

5.2 Recommendations ……66

References …….....67

LIST OF TABLE

Table	Title	Page
4.1	Lithology and Aquifers Borehole log	50

LIST OF FIGURES

Figure	Title	Page
1.1	Physiographical map of Northern Nigeria	4
1.2	Map showing the Study Area	5
1.3	Geological Map of Shika and its surrounding Showing the Study Area	7
1.4	Simplified Geological Map of Nigeria	8
2.1	A Sketch Showing the Principle of DC Resistivity Measurement	17
2.2	Typical ranges of electric resistivities of Geologic Materials	24
2.3	Current flowing through Cylindrical Model	25
2.4	An Electrode Configuration	27
3.1	ABEM LUND Imaging System	32
3.2	An enlarged Map of the Study Area Showing Profiles Layout around the dam	33
3.3	An Arrangement of electrodes for a 2D Electrical Survey	35
3.4	Common Arrays used in Resistivity Surveys and their Geometric Factors	37
3.5	Measurement Procedure with Wenner Array	44
4.1	Arrangement of Model Blocks and Apparent Resistivity Datum Points	47
4.2	A Profile showing Example of a Data Set with a few Bad Data Points	49
4.3	An Example of a Wenner Pseudo –Section	53

4.4a Measured apparent Resistivity Pseudosection (b) calculated Apparent Resistivity Pseudosection and (c) Inverse Model Resistivity Section for Profile one 55

4.5a. Measured apparent Resistivity Pseudosection (b) calculated Apparent Resistivity Pseudosection and (c) Inverse Model Resistivity Section for Profile Two 57

4.6a. Measured apparent Resistivity Pseudosection (b) calculated Apparent Resistivity Pseudosection and (c) Inverse model Resistivity Section for Profile Three..... 59

4.7a. Measured apparent Resistivity Pseudosection (b) calculated Apparent Resistivity Pseudosection and (c) Inverse model Resistivity Section for Profile Four 61

4.8a. Measured apparent Resistivity Pseudosection (b) calculated Apparent Resistivity Pseudosection and (c) Inverse model Resistivity Section for Profile Five 63

CHAPTER ONE

INTRODUCTION

1.1 General

A dam has its relevance in supply of water for municipal and industrial use, human and animal consumption, generation of electrical power and irrigation.

The integrity of a dam can be undermined by the existence of geological features such as faults, fractures, fissures, jointed or shear zones. Precipitated seepage zones in the bedrock and discontinuities in the structure itself are other factors that pose threat to the integrity of a dam.

In the past, geophysical methods were generally employed during dam – site feasibility studies involving foundation investigation, geological and structural mapping of both the dam axis and reservoir floor. These days however, the methods are also applied during and after the construction phase (Slimark and Djordjevic, 1987 and Buttler et. al, 1989)

The purpose of electrical surveys is to determine the subsurface resistivity distribution by making measurements on the ground surface. From these measurements, the true resistivity of the subsurface can be estimated. The ground resistivity is related to various geological parameters such as the mineral and fluid contents, porosity and degree of water saturation in the rock. Electrical resistivity surveys have been used

for many decades in hydrogeological, mining and geotechnical investigations. It is routinely used in engineering and hydrogeological investigations to investigate the shallow subsurface geology (Kearey and Breaks, 1996).

In environmental applications, resistivity surveys are capable of mapping overburden depth, stratigraphy, faults, fractures, rock units, salt water intrusion, contamination plumes, waste dumps, and voids. In geotechnical applications, resistivity surveys are used for dam stability studies, bedrock strength, mapping overburden, and faults and fractures.

The resistivity method has its origin in the 1920's due to the work of the Schlumberger brothers. For approximately the next 60 years, for quantitative interpretation, conventional sounding surveys (Koefoed, 1979) were normally used. In this method, the centre point of the electrode array remains fixed, but the spacing between the electrodes is increased to obtain more information about the deeper sections of the subsurface. Because of the limitation of the resistivity sounding method which does not take into account the horizontal changes in the subsurface resistivity, a more accurate model of the subsurface, two-dimensional resistivity imaging, where the resistivity changes in the vertical direction as well as in the horizontal direction along the survey line was employed in this research work.

In two-dimensional model, it is assumed that resistivity does not change in the direction that is perpendicular to the survey line. In many situations, particularly for surveys over elongated geological bodies, this is a reasonable assumption. In theory, a 3-D resistivity survey and interpretation model should be even more accurate. However, at present time, 2-D surveys are the most practical economic compromise between obtaining very accurate results and keeping the survey costs down.

1.2 Climate and Geomorphology of Study Area

Bomo dam is situated along Zaria – Funtua – Sokoto Road, North of ABU main campus. It falls within the high plains of Hausa land (fig 1.1), which stretches East –West from Lake Chad to Sokoto basin. The dam is bounded by IAR farm in the south and Bomo village in the North and East. (Fig. 1.2)

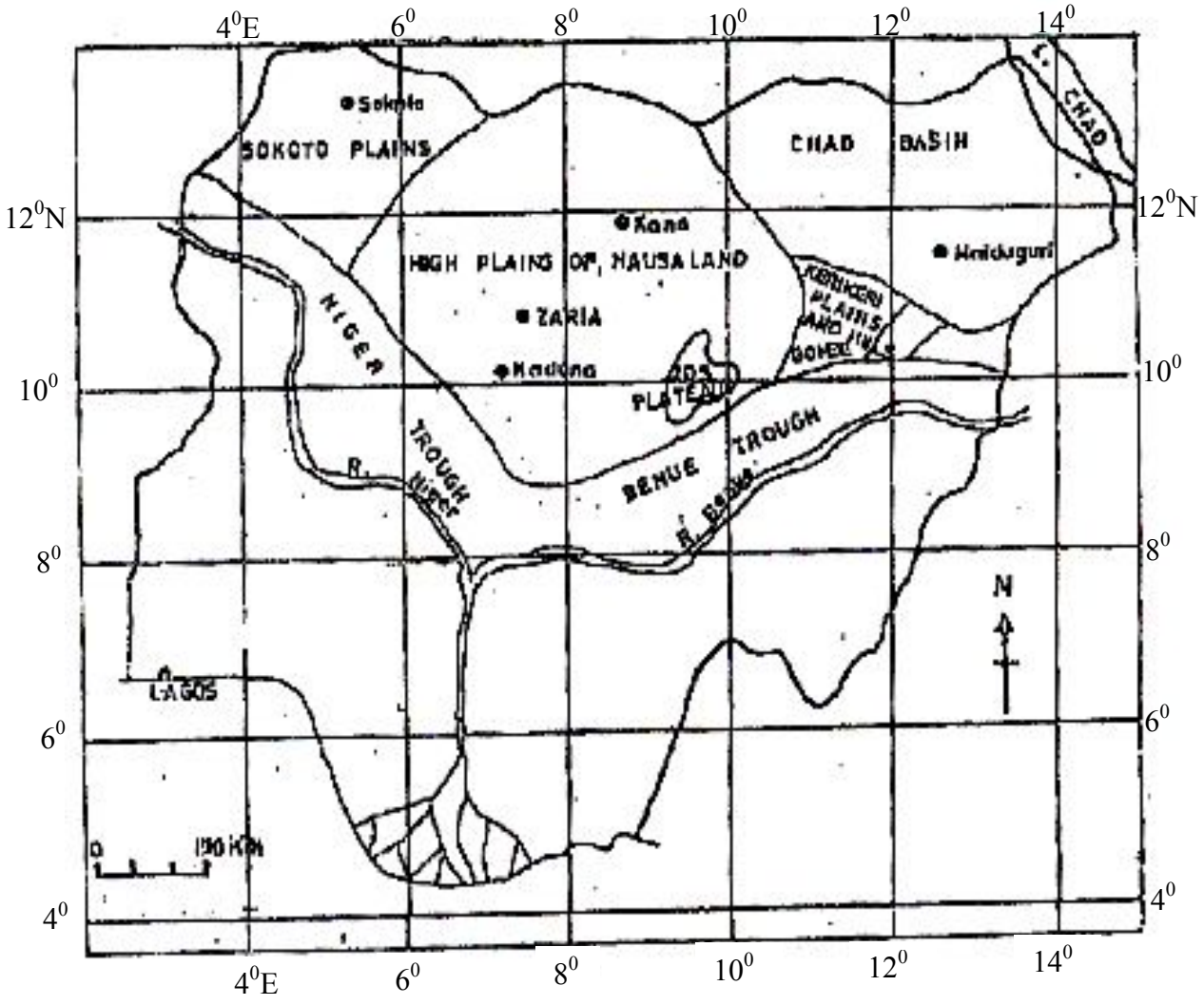


Figure 1.1 Physiographical Map of Northern Nigeria (Courtesy of Geography Dept ABU)

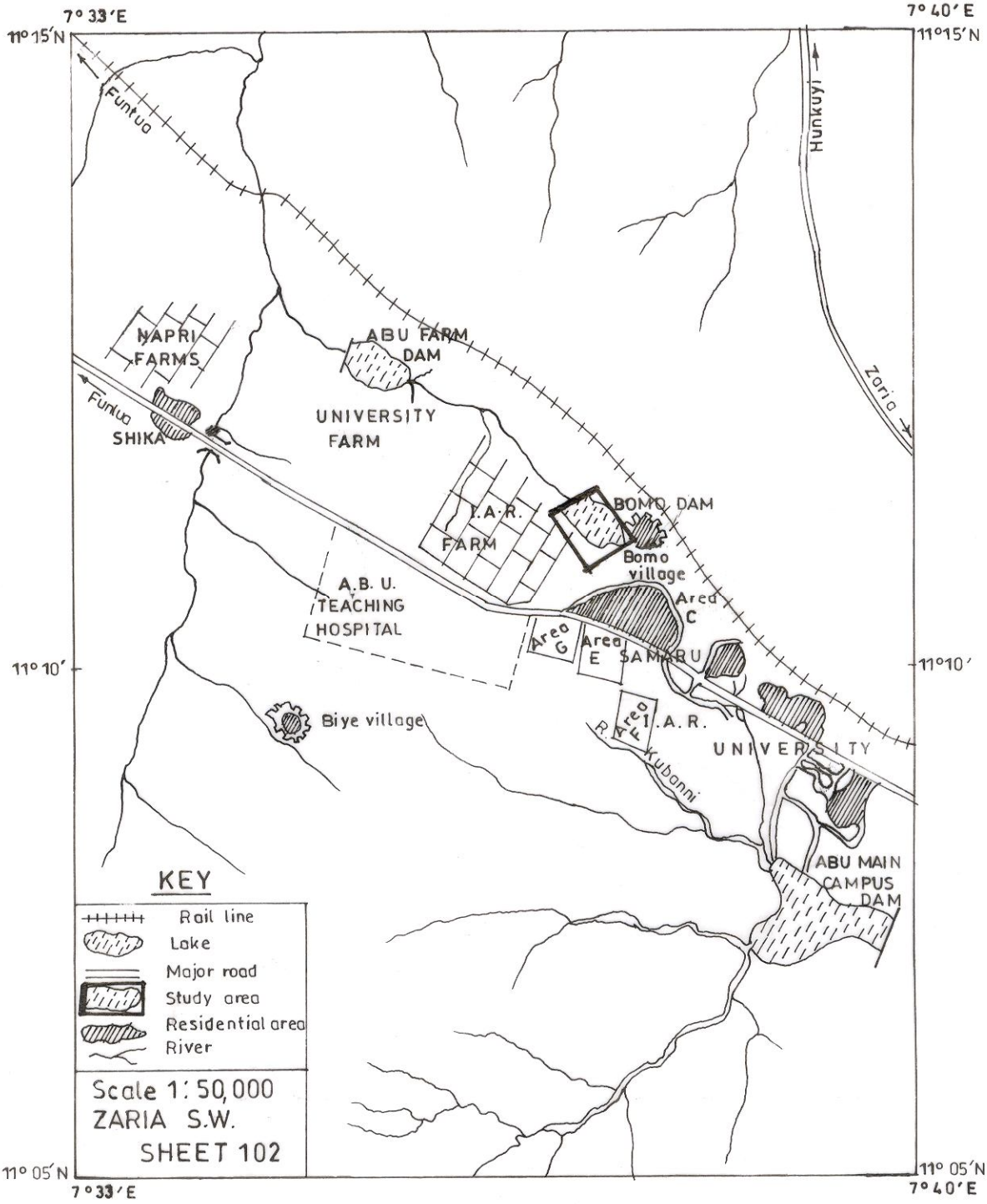


Figure 1.2 Map showing the study area

The area lies on latitude 11^0 11^1 N and longitude 7^0 37^1 E. It has an altitude of about 680m above the mean sea level. It has dry season from November to April and wet season from May to October. The annual rainfall is about 109cm (Hore, 1970).

1.3 General Geology of the Study Area

The study area falls under the Nigeria Basement complex underlain by Precambrian rocks. The geology of the study area is the same as that of the Nigerian Basement Complex (fig 1.3) The rocks typically found within the basement complex include gneisses, migmatites, metasediments and some intercalation of amphibolites.

The geology of Nigeria can be classified into two parts: The Basement Complex and the sedimentary Basins (fig 1.4).

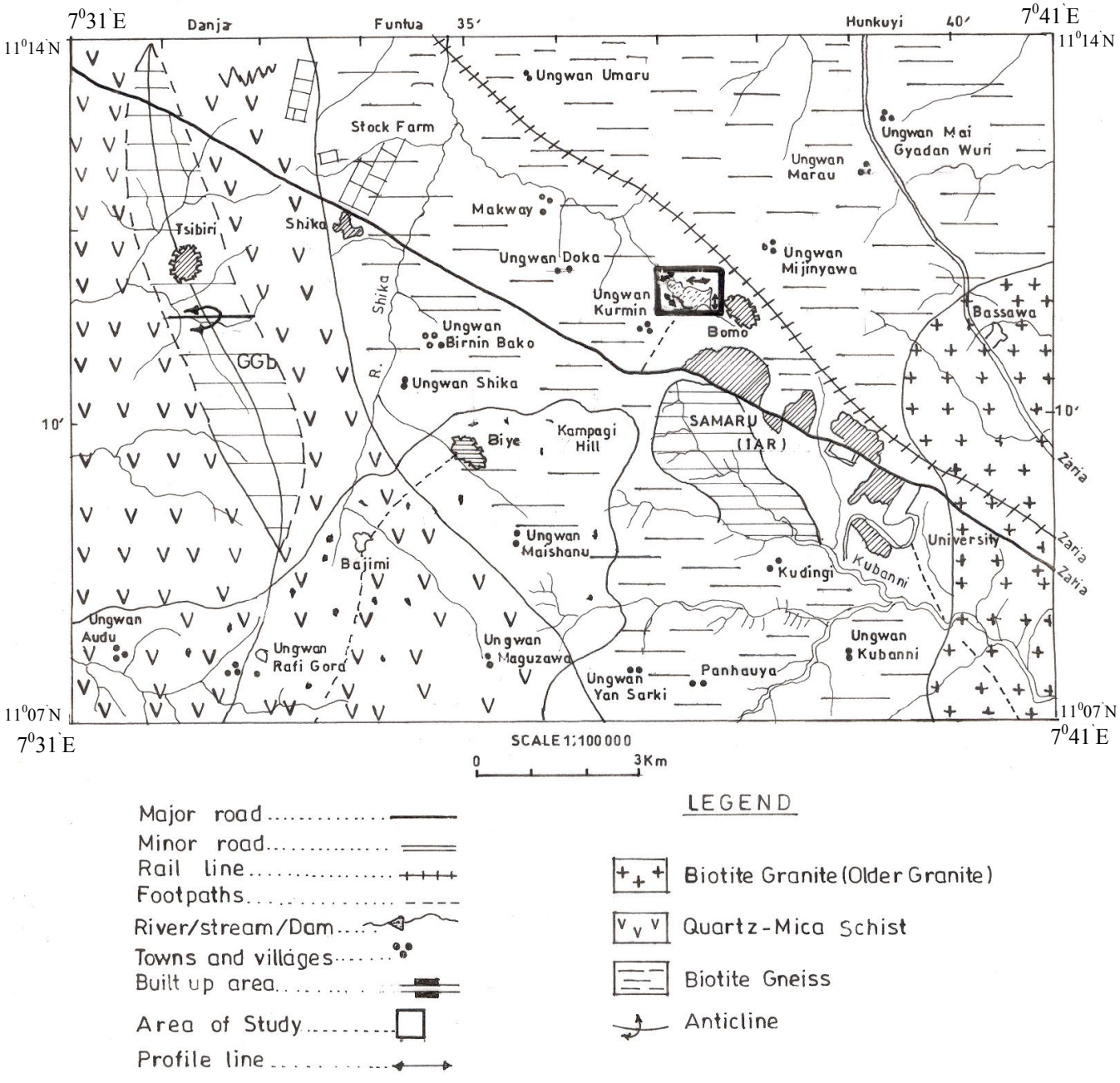


Figure 1.3 Geological Map of Shika and its surrounding showing the Study Area

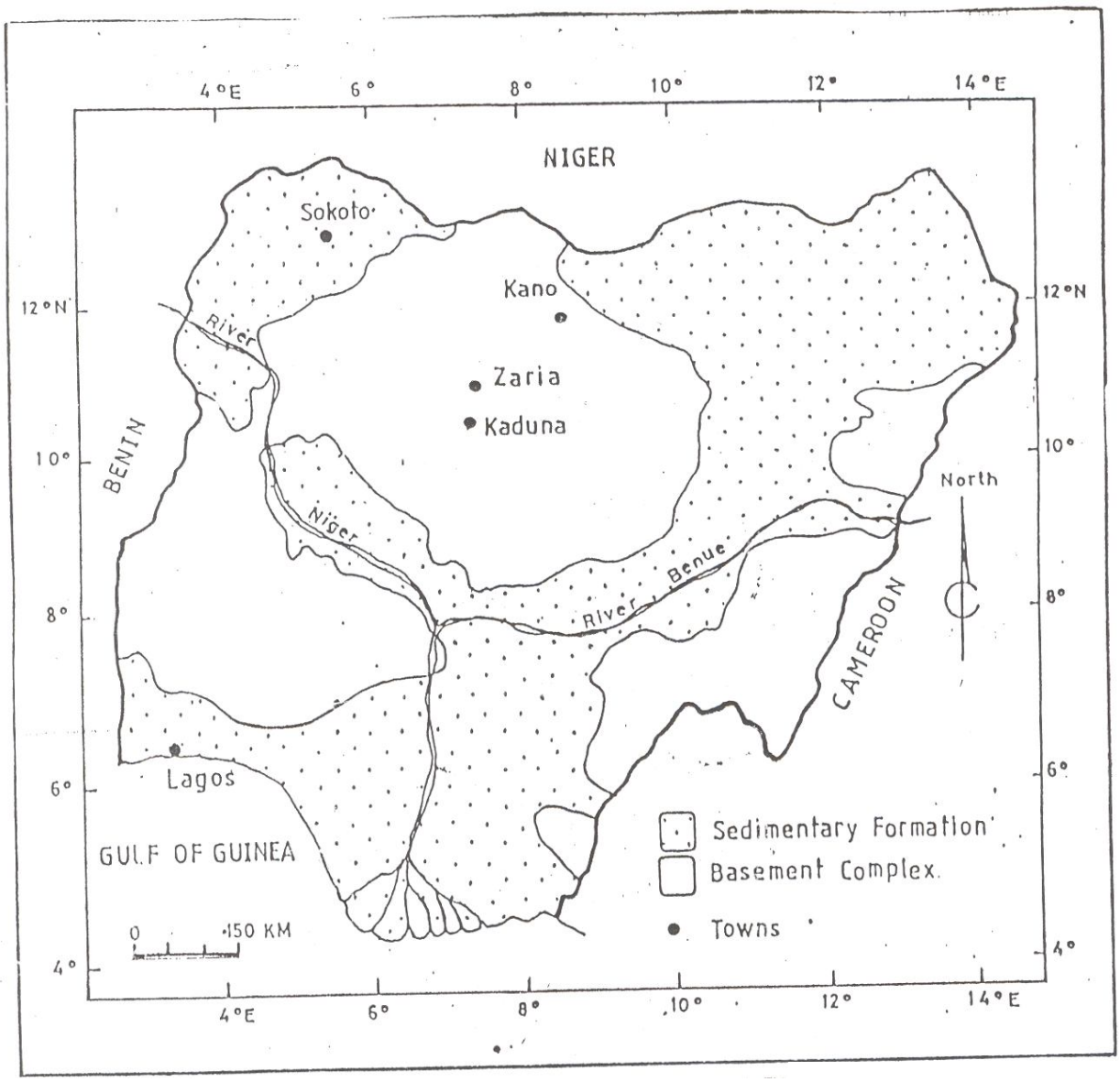


Figure 1.4 Simplified geological Map of Nigeria (Courtesy of G.S.N)

The rocks of the basement complex occupy more than 50% of the total land surface of Nigeria. The basement complexes accommodate the metasediments and are made up of gneisses. Exposures are scanty and highly weathered. The rock types are biotite, gneisses, granite gneisses and in parts with subordinate migmatites (McCurry, 1970).

The Basement Complex is divided into four broad groups, namely:-

(i) Older Metasediment

(ii) The Younger Metasediment

(iii) The Older Granite

(iv) The Younger Granite

1.3.1 The Older Metasediments

They are believed to be of Birrimian (greater than 100 million years) in age and rock types include gneisses, which have suffered at least two episodes of tectono – metamorphic deformations resulting in widespread occurrences of migmatitic and granitic gneisses (McCurry, 1970). It is overlain by igneous and metamorphic rocks of variable undifferentiated biotite and biotite – hornblende gneiss.

1.3.2 The Younger Metasediments

The younger metasediments are confined to the western half of Nigeria occurring as north – south trending belts. They are believed to have been deposited during the Katangan (800 to 1000 Ma) and folded along with the gneissic basement during the Pan African orogenic cycle. These metasediments once covered the whole older basement rocks and now have been removed by cycles of erosion, that they are preserved only in synclinal troughs.

The rock units within the metasedimentary belts include various kinds of schist phyllite, amphibolites, quartzites, metaconglomerates and calc – silicate rocks all of which are low to medium grade metamorphic rocks. The phyllites are the commonest in the northwestern parts while schist and amphibolites are dominant in the south-western parts.

1.3.3 The Older Granite

The Older Granite series comprises mainly granite Granodiorites, Diorites, Charnokitic rocks Syenites and Gabbros which intruded during the Pan – African orogenic cycle and formed part of the Precambrian basement complex. They sometimes occur as acid to basic complexes with the acidic types being later intrusions to the basic and intermediate types. Groups of volcanic rocks mainly agglomerates, tuffs, rhyolites, rhyodacites and dacities also occur associated with some of the acidic to basic complexes and believed to have been emplaced during

epeirogenic uplift at the closing stages of the Pan – African orogenic cycle.

1.3.4 The Younger Granite

The Younger Granite series are the ring complexes of Mesozoic (Jurassic) found in Northern Nigeria to have intruded the Precambrian to lower Palaeozoic basement rock. They are confined to zone stretching north – south of the Jos Plateau and extend to the Niger Republic with their ages progressively decreasing from Niger republic towards Nigeria with the youngest rocks found at the southern end of the ring complex. They are group of anorogenic rocks of Jurassic age (170 to 160 million years ago). Quite younger than the older Granite, but have equivalent composition. The major tectonic event that took place principally in the Jos Plateau around the Jurassic period resulted in the emplacement of the younger granites and associated rocks assemblage (Grant, 1969) outcrops occur as large masses and sometimes as ring dykes. Members include Rhyolite, Syenites and Gabbros.

1.4 Basement Geology around the Study Area

The study area falls within the Metasediments of the Basement Complex. The Basement Complex in Kaduna state was affected by an orogeny, which predated the emplacement of the Older Granites. During this event, deformation of the basement produced north – south

trending basins of Metasediment in the form of Synclinoria (Trustwell and Cope, 1963). Tertiary earth movements tilted the Metasediments to north and warped the basement along the axis of the uplift. Two of the Russ' axes of tertiary uplift pass through the present Kaduna state having northwest trend. They have a pronounced effect on the drainage pattern of the state.

1.5 General Hydrogeology

The climate and geology of an area are the major factors controlling the hydrogeology of that area. The geological formations underlying the area and their structures control the surface water and determine the type of aquifers to be formed and the means by which they are recharged. The climate, on the other hand determines the water content and the rate of recharge of the aquifer. Thus, the hydrogeology of the study area, like that of any other place is to a large extent, a function of the geologic and climatic setting. The climatic and the hydrogeologic conditions control the surface and the subsurface water in the area.

1.6 Review of Previous Study

The work by Akpoborie (1972), hydrogeological structures which control underground water in Samaru creeks, showed that structures

developed in rocks such as joints and fractures control the flow of groundwater into the creeks.

Wright and McCurry (1970) studied the basement geology of Zaria sheet 102 SW and concluded that the basement complex which covers the entire Zaria area is made up mostly of the older Granite and biotite – granite - gneiss

Ososami (1968) carried out vertical electrical sounding to investigate ground water potential in areas around A.B.U main campus, Samaru, Zaria. He revealed in his work that the depth to aquifer in the area varied from about 1m to about 30m. He however, could not clearly demarcate the boundary between the weathered basement and the fresh basement.

Farouq (2001) showed from his geoelectric investigation of the groundwater potential in the institute for Agricultural research farm Samaru, Zaria that the thickness of weathered basement around the area varied from about 3.4 m to about 30.4 m and the depth to fresh basement was about 40 m.

Hore (1970) noted that Zaria has tropical continental climate with prominence in the dry season around December and January. He confirmed the mean daily temperature of 31^0c reaching a maximum of about 36^0c around April with a mean annual rainfall of about 109cm.

Electrical resistivity imaging method was used by Christensen and Sorensen (1994) to map the lithology of the near-surface unconsolidated sediments and aquifers in the Grundfor area in Deanmark. The results obtained show that the low resistivity zones in the inversion model consist of more clayey quaternary glacial deposits while the high resistivity areas consist more sandy deposits. The model obtained was confirmed by a number of boreholes along the line.

The 2D electrical imaging survey carried out in Bauchi area of Nigeria by Acworth (1987) for groundwater exploration showed a thick weathered layer with fractures in the bedrock which are usually targets for groundwater.

Resistivity surveys were carried out along the seabed between Fisher Island and the mainland in Miami, Florida by Lagmansson (1998). The results obtained showed that the seabed consists of mud with a thickness of up to about 3 metres followed by sand overlying a sandstone and limestone bedrock which also contains cavities.

In the present study area (Bomo dam), however, no previous geophysical work has been done. As such the present study is meant to provide some geophysical information about the subsurface structure of the place.

1.7 Aim and Objectives

This research work is aimed at investigating the subsurface structure of Bomo dam with the following objectives:

To determine the thickness of the overburden.

To determine the thickness of the weathered basement.

To determine the nature of the fracture system.

To determine the texture of the strata underlying the dam.

CHAPTER TWO

PRINCIPLES AND THEORIES OF ELECTRICAL RESISTIVITY IMAGING

2.1 Introduction

The electrical resistivity imaging is a survey technique recently developed for the investigation of areas of complex geology where the use of resistivity sounding and other techniques is unsuitable (Griffiths and Barker, 1993). It involves measuring a series of constant separation traverses with the electrode spacing being increased with each successive traverse. Since increasing separation leads to greater depth penetration, the measured apparent resistivities may be used to construct a vertical contoured section displaying the variation of resistivity both laterally and vertically over the section.

The major limitation of the resistivity sounding method is that it does not take into account horizontal changes in the subsurface resistivity. A more accurate model of the subsurface is a two – dimensional (2-D) model where the resistivity changes in the vertical direction, as well as in the horizontal direction along the survey line. In this case, it is assumed that resistivity does not change in the direction that is perpendicular to the survey line. In many situations, particularly for surveys over elongated geological bodies, this is a reasonable assumption. In theory a 3-D resistivity survey and interpretation model should be even more accurate. However, at the present time, 2-D surveys are the most practical

economic compromise between obtaining very accurate results and keeping the survey costs down. Typical 1-D resistivity sounding surveys usually involve about 10 to 20 readings, while 2-D imaging surveys involve about 100 to 1000 measurements. In comparison, 3-D surveys usually involve several thousand measurements.

The cost of a typical 2-D survey could be several times the cost of a 1-D sounding survey, and is probably comparable with a seismic survey. In many geological situations, 2-D electrical imaging surveys can give useful results that are complementary to the information obtained by other geophysical method. For example, seismic methods can map undulating interfaces well, but will have difficulty (without using advanced data processing techniques) in mapping discrete bodies such as boulders, cavities and pollution plumes. Ground radar surveys can provide more detailed pictures but have very limited depth penetration in areas with conductive unconsolidated sediments, such as clayey soils.

2.2 Electrical Resistivity Method

The electrical resistivity method is based on measuring the potentials between one electrode pair while transmitting direct current (DC) between another electrode pair (fig 2.1) The depth of penetration is proportional to the separation between the electrodes, in homogeneous ground, and

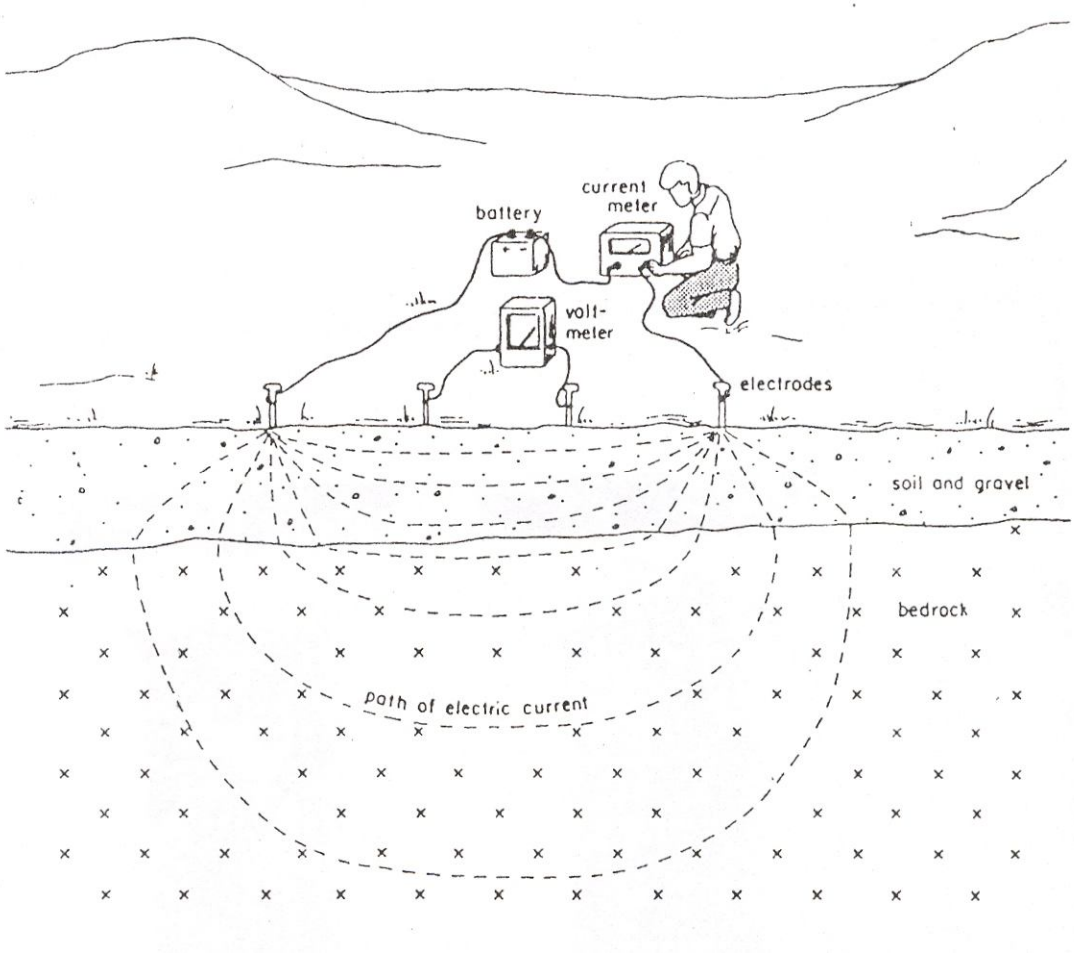


Figure 2.1 A Sketch Showing the Principle of DC Resistivity Measurement

varying the electrode separation provides information about the stratification of the ground. The measured quantity is called apparent resistivity. Interpreting the resistivity data consists of two steps: a physical interpretation of measured data, resulting in a physical model, and a geological interpretation of the resulting physical parameters.

The electrical resistivity surveys are used routinely in geothermal, mining, coal, groundwater and engineering applications (Keller and Frischknecht, 1966). In engineering application, electrical surveys are used for dam stability studies, bedrock strength, mapping overburden, faults and fracture.

There are three basic modes of operation for any resistivity method: sounding, profiling and sounding – profiling.

2.2.1 Vertical Electrical Sounding (VES)

This is also known as electrical drilling or expanding probe. It is used mainly in the study of horizontal or near – horizontal interfaces. In this method the current and potential electrodes are maintained at the same relative spacing and the whole spread is progressively expanded about a fixed central point. Consequently, readings are taken as the current reaches progressively greater depths.

The measured apparent resistivity values are normally plotted on a log – log graph paper. To interpret the data from such a survey, it is normally assumed that the subsurface consists of horizontal layers. In this

case, the subsurface resistivity changes only with depth, but does not change in the horizontal direction.

The most severe limitation of the resistivity sounding method is that horizontal or lateral changes in the subsurface resistivity are commonly found. Lateral changes in the subsurface resistivity will cause changes in the apparent resistivity values that might be, and frequently are, misinterpreted as changes with depth in the subsurface resistivity. In many engineering and environmental studies, the subsurface geology is very complex where the resistivity can change rapidly over short distances. The resistivity sounding method might not be sufficiently accurate for such situations. However, the technique is extensively used in geotechnical surveys to determine overburden thickness and also in hydrogeology to define horizontal zones of porous strata.

2.2.2 Constant Separation Traversing (CST)

This is also known as electrical profiling. It is used to determine lateral variations of resistivity. The current and potential electrodes are maintained at a fixed separation and progressively moved along a profile. This gives some information about lateral changes in the subsurface resistivity, but cannot detect vertical changes in the resistivity. This method is employed in mineral prospecting to locate faults or shear zones and to detect localized bodies of anomalous conductivity. It is also used in geotechnical surveys to determine variations in bedrock depth

and the presence of steep discontinuities. Results from a series of CST traverses with a fixed electrode spacing can be employed in the production of resistivity contour maps.

The most useful method is a combination of sounding and profiling which delineates both lateral and vertical variations in resistivity. This is the method employed in electrical imaging.

2.3 Factors Affecting Electrical Resistivity

The electrical resistivity of rocks and minerals is an extremely variable property and depends on a number of factors. Bulk resistivities from the surface to more than 15km depth in a normal crust are controlled by aqueous electrolytic conduction by way of pores, fractures, faults, and shear zones. The Resistivity of crystalline rock formations such as granulites, granite, and diorite in situ is largely dependent upon the water in the fissures and fractures. Similarly, the porosity, degree of saturation and the nature of pore-electrolytes govern the resistivity of rocks like sandstone and limestone. A slight increase in resistivity with depth is the result of decreasing pore, fracture, fault and shear-zone porosity due to increased lithostatic load.

2.3.1 Water Salinity

Conduction in near-surface rocks is largely electrolytic, taking place in connected pore spaces, along grain boundaries, in fractures, faults and

shear zones but negligibly through the silicate framework. The ions which conduct the current result from the dissociation of salts, such dissociation occurring when salts are dissolved in water. Since each ion is able to carry only a definite quantity of charge, it follows that the more ions that are available in a solution the greater will be the charge that can be carried. Hence, the solution with the larger number of ions will have the higher conductivity. In general, for a given porosity, a rock which contains saline water within its pores will have a greater conductivity when the salinity of the water is high than when it is low. Resistivity decreases with increase in salinity.

2.3.2 Porosity of Rock

Porosity can be defined as the ratio of the percentage of the volume of void space to the total volume of the rock. Porosity arises from the fact that the particles do not occupy all the possible space. It provides a direct measure of the total void space available for the storage of fluids (Clark, 1960).

Resistivity and porosity in sedimentary rocks can be related by the general form of Archie's law, which for rocks devoid of clay is written as

$$F = \frac{\ell_r}{\ell_s} = a\phi^{-m}$$

Where F is the formation resistivity factor, ℓ_r is the resistivity of the rock, ℓ_s is the resistivity of the solution in the pores of the rock, ϕ is porosity, while

"a" and "m" are constants peculiar to the rock type. The constant "m" is usually referred to as the cementation factor while the constant "a" is referred to as the coefficient of saturation.

The most common minerals forming soils and rocks have very high resistivity in a dry condition, and the resistivity of soils and rocks is therefore normally a function of the amount and quality of water in pore spaces and fractures. The degree of connection between the cavities is also important.

2.3.3 Effect of Temperature

An increase in temperature lowers the viscosity of water, with the results that ions in the water become more mobile. The increased mobility of the ions results in an observed resistivity decrease with increase in temperature according to the formula (Keller and Frischknecht, 1966):

$$\ell_r = \frac{\ell_{18}}{1+\alpha(t-18)}$$

Where ℓ_r is the resistivity at this temperature, ℓ_{18} is the resistivity at 18^0c, α is the temperature coefficient of resistivity (about 0.025 per degree centigrade) and t is the ambient temperature.

2.3.4 Effects of Rock Texture and Porosity

The texture of a rock dictates its resistivity in the following ways:

(i) A well – sorted sandstone has large void spaces and hence exhibits low resistivity.

(ii) A poorly - sorted sandstone will have a much lower porosity and hence will exhibit higher resistivity.

(iii) Dissolution along fractures in a limestone will enhance porosity and hence lower resistivity.

(iv) Precipitation of some minerals in any rock will lower the porosity and hence increase resistivity.

(v) Basalt has much unconnected or dead-end pore space and hence low permeability, so that even basalt of high porosity may exhibit high resistivity.

2.3.5 Effects of Geological Processes

In general, geological processes reduce the resistivity of a rock but there are exceptions.

Weathering or hydrothermal alteration of a granite significantly lowers its resistivity. Dissolution, faulting and shearing usually increase porosity and fluid permeability, and hence lower resistivity. Precipitation of calcium carbonate and silica reduces porosity and hence reduce fluid permeability and increase resistivity. Induration by compaction or metamorphism will reduce porosity and permeability and hence increase resistivity. Salt water intrusion provides more ions for conduction and therefore reduces resistivity.

2.3.6 Effect of Rock type

Figure 2.2 displays the typical ranges of resistivities for a number of rock and soil types. These ranges in part reflect the textural types and the

effects of the geological processes. The resistivity of a type of soil or rock may vary widely. However, the variation may be more limited within a confined geological area and variations in resistivity within a certain soil or

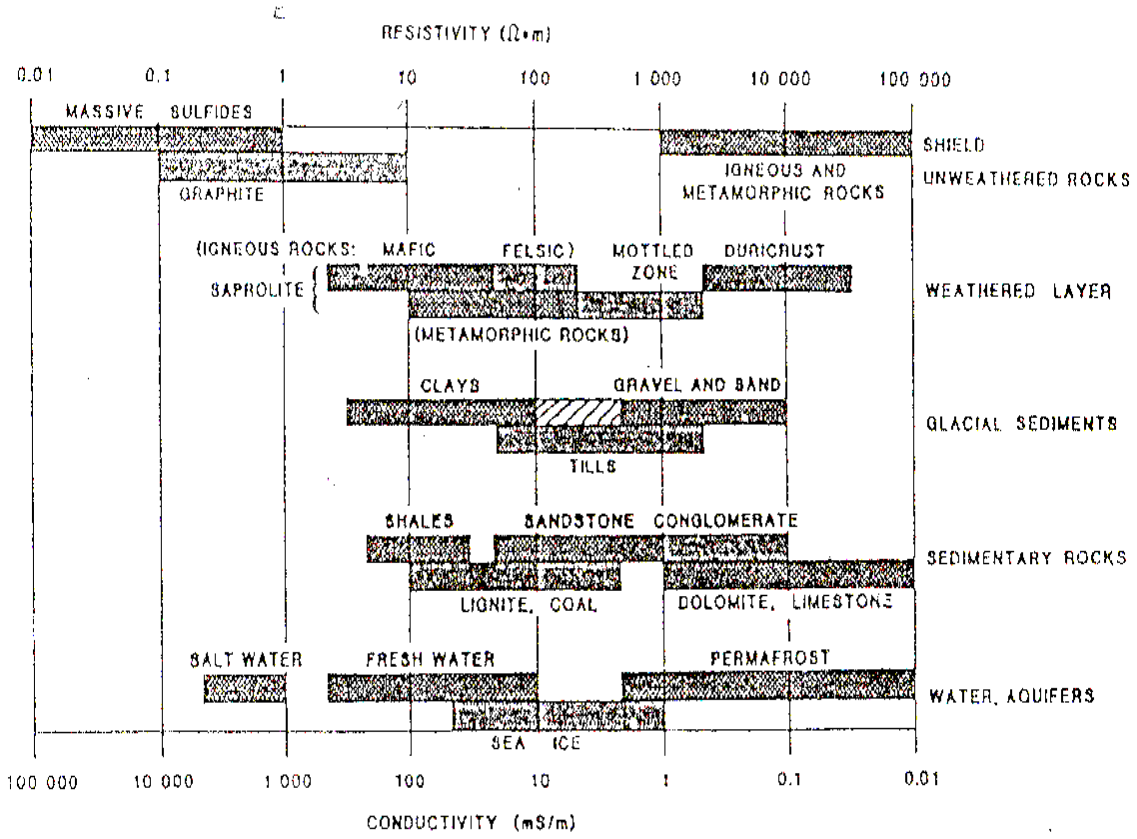


Figure 2.2 Typical ranges of electric resistivities of geologic materials (ABEM INSTRUCTION MANUAL)

rock type will reflect variations in physical properties. For example, the lowest resistivities encountered for sandstones and limestones mean that the pore spaces in the rock are saturated with water, whereas the highest values represent strongly consolidated sedimentary rock or dry rock above the groundwater surface. The large ranges and overlap of these ranges for the resistivity of the various rock types make rock type identification by resistivity difficult.

2.4 Theory of the D.C Resistivity Method

The principle underlying the resistivity method is embodied in ohm's law.

Consider a current **I** flowing through a cylindrical object of length **L** (fig. 2.3)

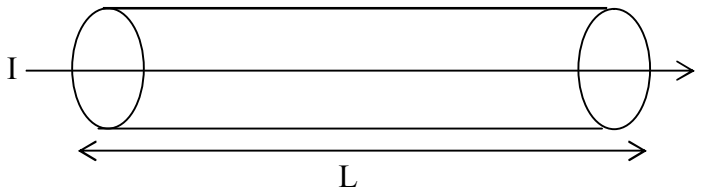


Fig 2.3 Current flowing through Cylindrical Model

$$R \alpha \frac{L}{A} \quad \text{..... (2.1)}$$

$$R = \frac{\rho L}{A} \quad \text{..... (2.2)}$$

Where Δ is a constant of proportionality called resistivity.

From ohm's law

$$R = \frac{\Delta V}{I} \quad \text{..... (2.3)}$$

Combining equation (2.2) and (2.3)

$$\frac{\rho L}{A} = \frac{\Delta V}{I} \quad \text{..... (2.4)}$$

$$\rho = \frac{A \Delta V}{IL} \quad \text{..... (2.5)}$$

Where Δ = resistivity (Σ m)

A = cross – section area (m^2)

)V = potential difference (V)

I = current (A)

L = length (m)

Resistivity Δ can be expressed in terms of electric field intensity E (V/m) and current density J (A/m^2)

$$\rho = \frac{E}{J} \quad \text{..... (2.6)}$$

(Since $E = \frac{\Delta V}{L}$ and $J = \frac{I}{A}$)

$$E = \frac{\rho I}{A} \quad \text{..... (2.7)}$$

For a sphere

$$E = \frac{\rho I}{4 \pi r^2} \quad \text{..... (2.8)}$$

$$E = -\nabla V = -\frac{dV}{dr} \quad \text{.....(2.9)}$$

$$V = -\int_r^{\infty} E \, dr \quad \text{..... (2.10)}$$

$$V = \frac{\rho I}{4 \pi r} \quad \text{..... (2.11)}$$

For hemisphere

$$V = \frac{\rho I}{2\pi r} \quad \text{..... (2.12)}$$

Consider four electrodes - two current electrodes C_1 and C_2 and two potential electrodes, P_1 and P_2 placed on earth surface as shown in (fig 2.4).

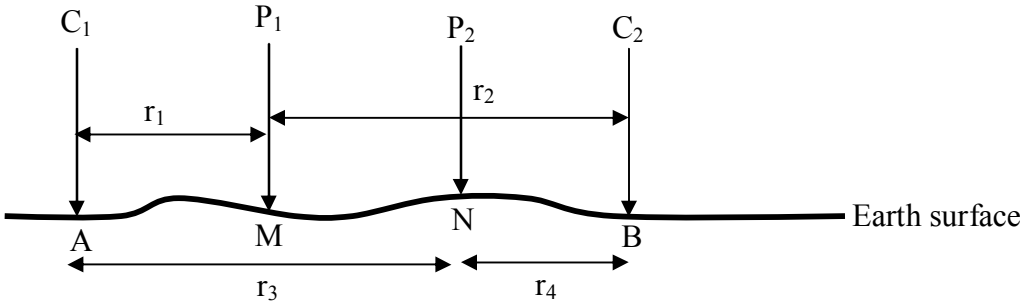


Figure 2.4 An electrode Configuration

Potential at P_1 due to C_1

$$V_M^A = \frac{I\rho}{2\pi r_1} \quad \text{..... (2.13)}$$

Potential at P_1 due to C_2

$$V_M^B = \frac{-I\rho}{2\pi r_2} \quad \text{..... (2.14)}$$

Potential at P_1 due to C_1 and C_2

$$V_M^{A,B} = \frac{I\rho}{2\pi}\left[\frac{1}{r_1} - \frac{1}{r_2}\right] \quad \text{..... (2.15)}$$

Potential at P_2 due to C_1

$$V_N^A = \frac{I\rho}{2\pi r_3} \quad \text{..... (2.16)}$$

Potential at P_2 due to C_2

$$V_N^B = -\frac{I\rho}{2\pi r_4} \quad \text{..... (2.17)}$$

Potential at P_2 due to C_1 and C_2

$$V_N^{A,B} = \frac{I\rho}{2\pi}\left[\frac{1}{r_3} - \frac{1}{r_4}\right] \quad \text{..... (2.18)}$$

Potential difference,)V between P_1 and P_2 due to C_1 and C_2

$$\Delta V = \frac{I\rho}{2\pi}\left[\frac{1}{r_1} - \frac{1}{r_2}\right] - \frac{I\ell}{2\pi}\left[\frac{1}{r_3} - \frac{1}{r_4}\right] \quad \text{.....} \quad \text{(2.19)}$$

Thus generally, the potential difference between two arbitrarily located points on the surface of a homogeneous isotropic ground is given by the expression:

$$\Delta V = \frac{I\rho}{2\pi}\left[\frac{1}{r_1} - \frac{1}{r_2} - \frac{1}{r_3} + \frac{1}{r_4}\right] \quad \text{..... (2.20)}$$

Where ρ is the resistivity, I is the current and r_1 r_2, r_3 and r_4 are the inter-electrode distance.

$$\rho = \frac{\Delta V}{I}\frac{2\pi}{\left[\left(\frac{1}{r_1} - \frac{1}{r_2}\right) - \left(\frac{1}{r_3} - \frac{1}{r_4}\right)\right]} \quad \text{..... (2.21)}$$

$$\rho = k\frac{\Delta V}{I} \quad \text{..... (2.22)}$$

Where $k = \dfrac{2\pi}{\left(\frac{1}{r_1} - \frac{1}{r_2}\right) - \left(\frac{1}{r_3} - \frac{1}{r_4}\right)}$ ..... (2.23)

K is known as geometric factor and it depends on the type of electrode array used.

For an inhomogeneous medium the calculated resistivity is called the apparent resistivity ℓa

$$\rho_a = \frac{\Delta V}{I} \frac{2\pi}{\left(\frac{1}{r_1} - \frac{1}{r_2} - \frac{1}{r_3} + \frac{1}{r_4}\right)} \quad \ldots\ldots\ldots\ldots\ldots\ldots\ldots\ldots\ldots\ldots\ldots\ldots\ldots\ldots \text{(2.24)}$$

The result is independent of the position of the electrodes and is not affected when the current and the potential electrodes are interchanged.

2.5 Concept of Apparent Resistivity

Most resistivity techniques define a response function called apparent resistivity, ρ_a which can be estimated from the surface measurements. These apparent resistivities are usually functions of a variable that is related to the depth of current penetration.

The apparent resistivity is equal to the true resistivity only when the subsurface is homogeneous. In practice, this condition is difficult to obtain. However, the subsurface is assumed to be divided into thin strata with each stratum regarded as completely homogeneous and isotropic (Koefoed, 1979). This is a convenient way of representing a response of the actual distribution of lateral resistivity in the subsurface on the basis of subsurface measurement. If the electrodes are laid out along a profile and their separations are increased systematically, the change in the apparent resistivity will be a function of electrode spacing.

2.6 Limitations of Electrical Resistivity Method

Resistivity surveying is an efficient method for delineating shallow layered sequences or vertical discontinuities involving changes of resistivity. It does, however, suffer from a number of limitations:

(1) Interpretations are ambiguous. Consequently, independent geophysical and geological controls are necessary to discriminate between valid alternative interpretations of the resistivity data.

(2) Interpretation is limited to simple structural configuration. Any deviations from these simple situations may be impossible to interpret.

(3) Topography and the effects of near-surface resistivity variations can mask the effects of deeper variations.

(4) The depth of penetration of the method is limited by the maximum electrical power that can be introduced into the ground and by the practical difficulties of laying out long lengths of cable.

CHAPTER THREE

FIELD SURVEY METHOD AND INSTRUMENTATION

3.1 Introduction

The ABEM Lund Imaging system ((fig 3.1) was used for the data acquisition. It consists of:

ABEM Terrameter SAS 4000

ABEM Electrode Selector ES464, including connectors to Terrameter (serial port and current / voltage terminals)

ABEM SAS External Battery Adaptor (EBA)

Reels of Cables

Electrodes and Jumpers

For this research work, two reels of cables were used. The electrodes, numbering 42 were placed at intervals of 5m. However, the two innermost electrodes adjoining the two reels of cables coincided, thus yielding a total of 41 electrodes and a spread length of 200m. A total number of five profiles were laid along the periphery of the dam (fig. 3.2). Some were oriented parallel and, in some cases, perpendicular to the axis of the dam. The data obtained for each profile were processed using RES2DIVN software.

The modern field systems such as the Lund imaging system (Terrameter SAS 4000) use a multicore cable to which 24 or more electrodes are connected at takeouts moulded on at predetermined equal intervals. Such a cable is very much like a seismic cable and is used

in a similar way. The cable is connected to a switching module and to an earth resistance meter and computer through an RS232 port. With



Figure 3.1 ABEM LUND IMAGING SYSTEMS

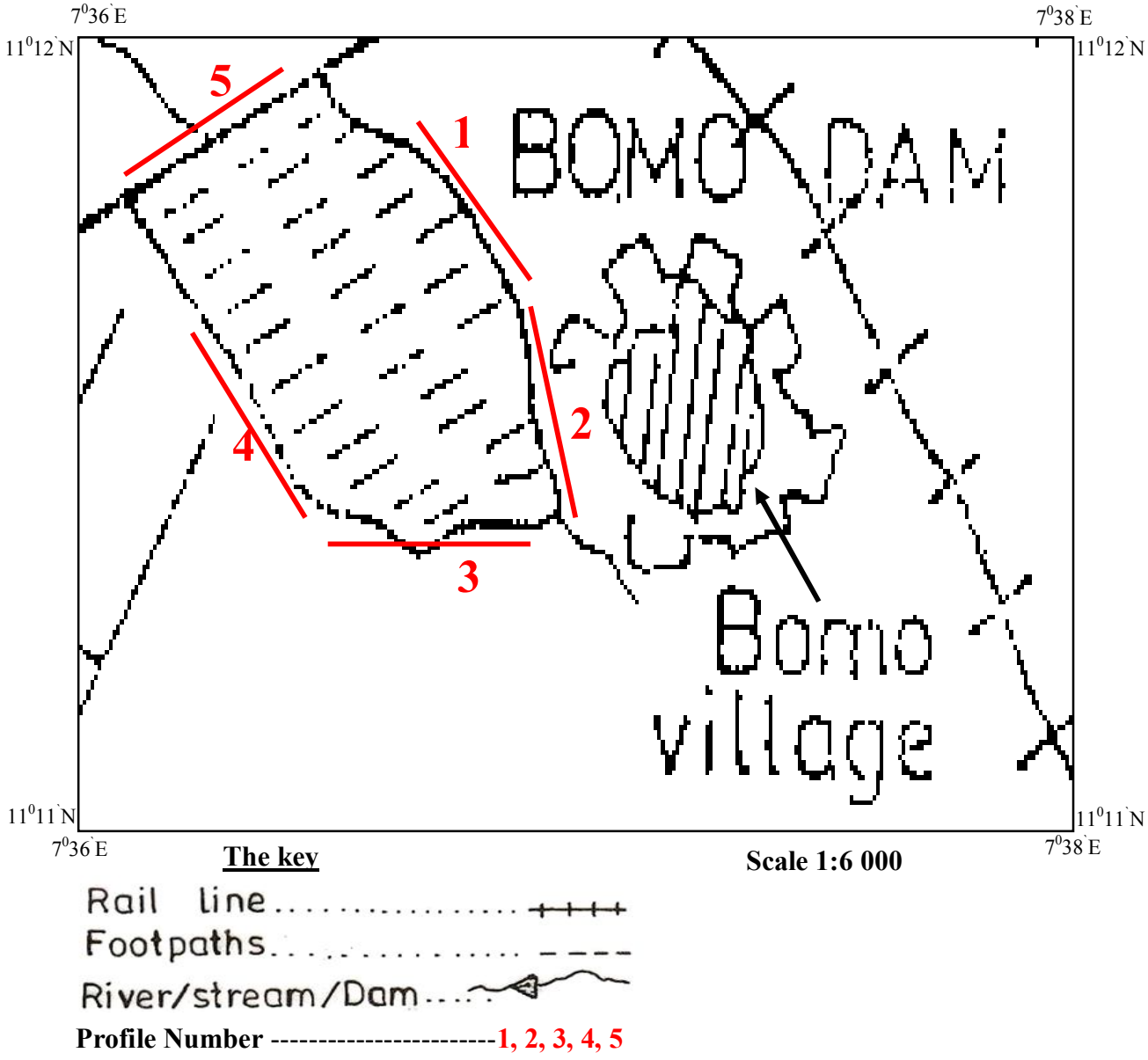


Figure 3.2: An Enlarged Map of the Study Area showing the Profiles Layout around the Dam.

these systems, any electrodes may be switched to act as either current or potential electrodes and so within the constraints of the electrodes emplaced, any electrode arrangement can be employed. In practice either the two-electrode (pole-pole), Wenner, pole-dipole or dipole – dipole are employed.

The advent of automated data acquisition and inversion in recent years has increased the practical applicability of resistivity imaging tremendously. One of the new developments in recent years is the use of 2D electrical imaging surveys to map areas with moderately complex geology (Griffiths and Barker, 1993). Computer – controlled data acquisition systems generally consists of a resistivity instrument, a relay switching unit, a computer, electrode cables, various connectors and electrodes.

In the field survey, the electrode cables are rolled out and electrodes are connected to it (fig 3.3), after which the data acquisition software automatically checks the electrode contact and scans through a pre-defined measurement protocol. A laptop microcomputer together with an electronic switching unit is used to automatically select the relevant four electrodes for each measurement.

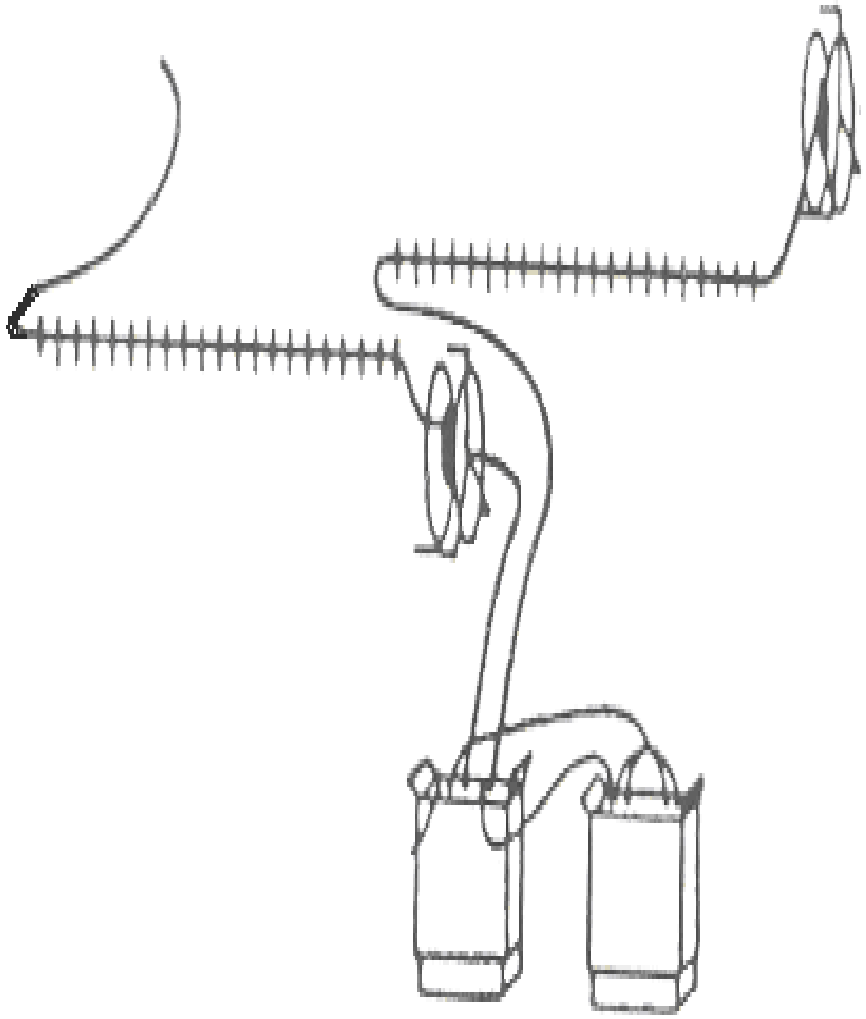


FIGURE 3.3 AN ARRANGEMENT OF ELECTRODES FOR A 2 D ELECTRICAL SURVEY

3.2 Electrode Arrays

Many configuration of electrodes have been designed (Habberjam 1979). Figure 3.4 shows some common electrode arrays used in resistivity survey. C_1 and C_2 are the positions of current electrodes while P_1 and P_2 are the position of potential electrodes. The choice of the best array for a field survey depends on the type of structure to be mapped, the sensitivity of the resistivity meter and the background noise level. In practice, the arrays that are most commonly used for 2 – D imaging surveys are:-

i) Wenner
ii) Dipole-Dipole
iii) Wenner – Schlumberger
iv) Pole – Pole
v) Pole – Dipole

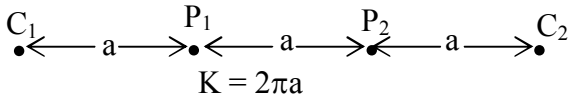
Some of the characteristics of array that are considered for field survey are:-

(i) The sensitivity of the array to vertical and horizontal changes in the subsurface resistivity.
(ii) The depth of investigation
(iii) The horizontal data coverage
(iv) The signal strength
(v) Sensitivity to surficial inhomogeneties
(vi) Electromagnetic coupling

3.2.1 Wenner Array

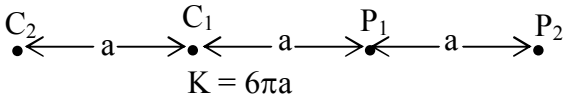
In the wenner array the separation between adjacent electrodes are equal to each other and the apparent resistivity ρ_a is given by:

(a) **Wenner Alpha**



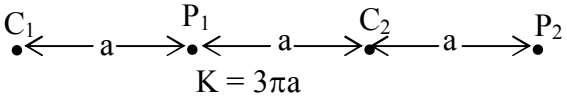
$K = 2\pi a$

(b) **Wenner Beta**



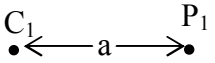
$K = 6\pi a$

(c) **Wenner Gamma**



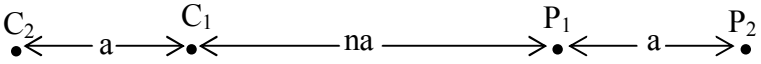
$K = 3\pi a$

(d) **Pole - Pole**



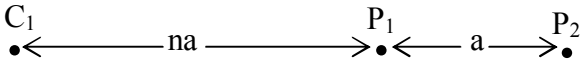
$K = 2\pi a$

(e) **Dipole - Dipole**



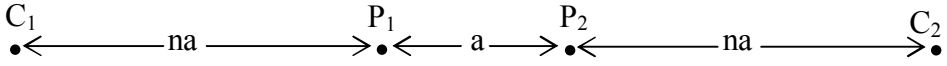
$K = \pi n (n + 1) (n + 2) a$

(f) **Pole - Dipole**



$K = 2\pi n (n + 1) a$

(g) **Wenner - Schlumberger**



$K = \pi n (n + 1) a$

Figure 3.4 Common Arrays used in Resistivity Surveys and their Geometric Factors

$$\rho_a = 2\pi\, a\,.\frac{\Delta V}{I} \quad \text{..... (3.1)}$$

Where a = Uniform electrode separation

$2\pi a$ = Geometric factor.

ΔV = Potential difference

I = Current

The wenner array is relatively sensitive to vertical changes in the subsurface resistivity below the centre of the array. However, it is less sensitive to horizontal changes in the subsurface resistivity. In general, the wenner is good in resolving vertical changes (i.e. horizontal structure), but relatively poor in detecting horizontal changes (i.e. narrow vertical structures). Among the common arrays, the Wenner array has the strongest signal strength. This can be an important factor if the survey is carried out in areas with high background noise. One disadvantage of this array for 2-D surveys is the relatively poor horizontal coverage as the electrode spacing is increased.

3.2.2 Dipole-Diple Array

This array is widely used in resistivity / I.P surveys because of the low Electromagnetic coupling between the current and potential circuits. The spacing between the current electrode pair, $C_2 - C_1$, is given as "a" which is the same as the distance between the potential electrodes pair $P_1 - P_2$. The factor "n" is the ratio of the distance between the C_1 and P_1 electrodes to the $C_2 - C_1$ or $P_1 - P_2$ dipole separation "a". For surveys

with this array, the "a" spacing is initially kept fixed and the "n" factor is increased from 1 to 2 to 3 until up to about 6 in other to increase the depth of investigation.

The dipole – dipole array is very sensitive to horizontal changes in resistivity, but relatively insensitive to vertical changes in the resistivity. It is good in mapping vertical structures, such as dykes and cavities, but relatively poor in mapping horizontal structures such as sedimentary layers. The apparent resistivity, ρ_a is given by:

$$\rho_a = \pi\, n(n+1)(n+2)a.\frac{\Delta V}{I} \quad \text{..... (3.2)}$$

In general, this array has a shallower depth of investigation compared to the wenner array. However, for 2-D surveys, this array has a better horizontal data coverage than the wenner.

Another possible disadvantage of this array is the very small signal strength for large values of the "n" factor.

3.2.3 Wenner – Schlumberger Array

This is a new hybrid between the wenner and Schlumberger arrays (Pazdirek and Blaha 1996) arising out of relatively recent work with electrical imaging surveys. The array is moderately sensitive to both horizontal and vertical structures. In areas where both types of geological structures are expected, this array might be a good compromise between the Wenner and the dipole-dipole arrays. The signal strength for this array

is smaller than that of the Wenner array but higher than the dipole-dipole array.

The Wenner – Schlumberger array has a slightly wider horizontal data coverage than the Wenner array, but narrower than that obtained with the dipole-dipole array.

The apparent resistivity, ρ_a is given by:

$$\rho_a = \pi n(n+1)a.\frac{\Delta V}{I} \quad \text{..... (3.3)}$$

The "n" factor is the ratio of the distance between the $C_1 - P_1$ or $P_2 - C_2$ electrodes to the spacing between the P_1- P_2 potential pair.

3.2.4 Pole-Pole Array

This array is not as commonly used as the Wenner, dipole-dipole and Schlumberger arrays. In practice the ideal pole-pole array, with one current and one potential electrode does not exist. To approximate the pole-pole array, the second current and potential electrodes (C_2 and P_2) must be placed at a distance which is more than 20 times the maximum separation between C_1 and P_1 electrodes used in the survey. The effect of the C_2 or P_2 electrode is approximately proportional to the ratio of the $C_1 - P_1$ distance to the $C_2 - P_1$ distance. If the effects of the C_2 and P_2 electrodes are not taken into account, the distance of these electrodes from the survey line must be at least 20 times the largest C_1 - P_1 spacing used to ensure that the error is less than 5%. In surveys where the inter-

electrode spacing along the survey line is more than a few meters, there might be practical problems in finding suitable locations for the C_2 and P_2 electrodes to satisfy this requirement.

Pole–pole array is popular in some applications such as archaeological surveys where small electrode spacings are used. It has the widest horizontal coverage and the deepest depth of investigation. However, it has the poorest resolution. Another disadvantage of this array is that because of the large distance between the P_1 and P_2 electrodes, it can pick up a large amount of telluric noise which can severely degrade the quality of the measurement.

The apparent resistivity ρ_a is given by:

$$\rho_a = 2\pi\, a . \frac{\Delta V}{I} \quad \text{..... (3.4)}$$

3.2.5 Pole-Dipole Array

The pole-dipole array also has relatively good horizontal coverage. It has a significantly higher signal compared with the dipole-dipole array and it is not as sensitive to telluric noise as the pole-pole array.

The pole-dipole array also requires a remote electrode, the C_2 electrode, which must be placed sufficiently far from the survey line. For the pole-dipole arrays, the effect of the C_2 electrode is approximately proportional to the square of ratio of the C_1 - P_1 distance to the C_2 - P_1 distance. Thus the pole-dipole array is less affected by the C_2 remote electrode

compared with the pole-pole array. If the distance of the C_2 electrode is more than 5 times the largest C_1 - P_1 distance used, the error caused by neglecting the effect of the C_2 electrode is less than 5%. The exact error also depends on the location of the P_2 electrode for the particular measurement and the subsurface resistivity distribution.

The signal strength is lower compared with the wenner and Wenner-Schlumberger arrays but higher than the dipole-dipole array. For IP surveys, the higher signal strength (compared with the dipole-dipole array) combined with the lower EM coupling (compared with the Wenner and Wenner-Schlumberger Arrays) due to the separation of the circuitry of the current and potential electrodes makes this array an attractive alternative.

The apparent resistivity ρ_a is given by:-

$$\rho_a = 2\pi n(n+1)a.\frac{\Delta V}{I} \quad \text{..... (3.5)}$$

3.3 The Measurement Procedure for Wenner Electrode Configuration

For this research work wenner electrode array was used since it is one of the most satisfactory array for imaging purposes (Griffiths and Barker 1993). Wenner pseudo-sections have some advantages over dipole-dipole pseudo-section, the most important of which is that wenner profiling data are less affected by near-surface resistivity variations which

on dipole–dipole pseudo-sections can cause strong distortions of the contours.

For a 2-D survey with a number of electrodes along a straight line attached to a multi-core cable, a constant spacing between the adjacent electrodes is used. The multi-core cable is attached to an electronic switching unit which is connected to a laptop computer. The sequence of measurements to take, the type of array to use and other survey parameters, such as the current to use, are normally entered into a text file which can be read by a computer program in a laptop computer. Different resistivity meters use different formats for the control file. After reading the control file, the computer program then automatically selects the appropriate electrodes for each measurement.

In a typical survey, most of the field work is in laying out the cable and electrodes. After that, the measurements are taken automatically and stored in the computer. Most of the survey time is spent waiting for the resistivity meter to complete the set of measurements.

To obtain a good 2-D picture of the subsurface, the coverage of the measurements must be 2-D as well. As an example, figure 3.5 shows a possible sequence of measurements for the wenner electrode array for a system with 20 electrodes. Here, measurement commences at one end of the line using electrodes 1, 2, 3 and 4. The spacing between the adjacent

electrodes is "a". With wenner array, the first step is to make all the possible measurement with an electrode spacing of "1 a".

Electrode 1 is used as the first current electrode C_1, electrode 2 as the first potential electrode P_1, electrode 3 as the second potential electrode P_2 and electrode 4 as the second current electrode C_2. For the second measurement, electrodes 2, 3, 4 and 5 are used for C_1, P_1, P_2, and C_2 respectively. This is repeated down the line of electrodes until electrodes 17, 18, 19 and 20 are used for the last measurements with "1a" spacing. The spacing is then doubled without moving on, the first active electrodes with "2a" electrode spacing being 1, 3, 5 and 7.

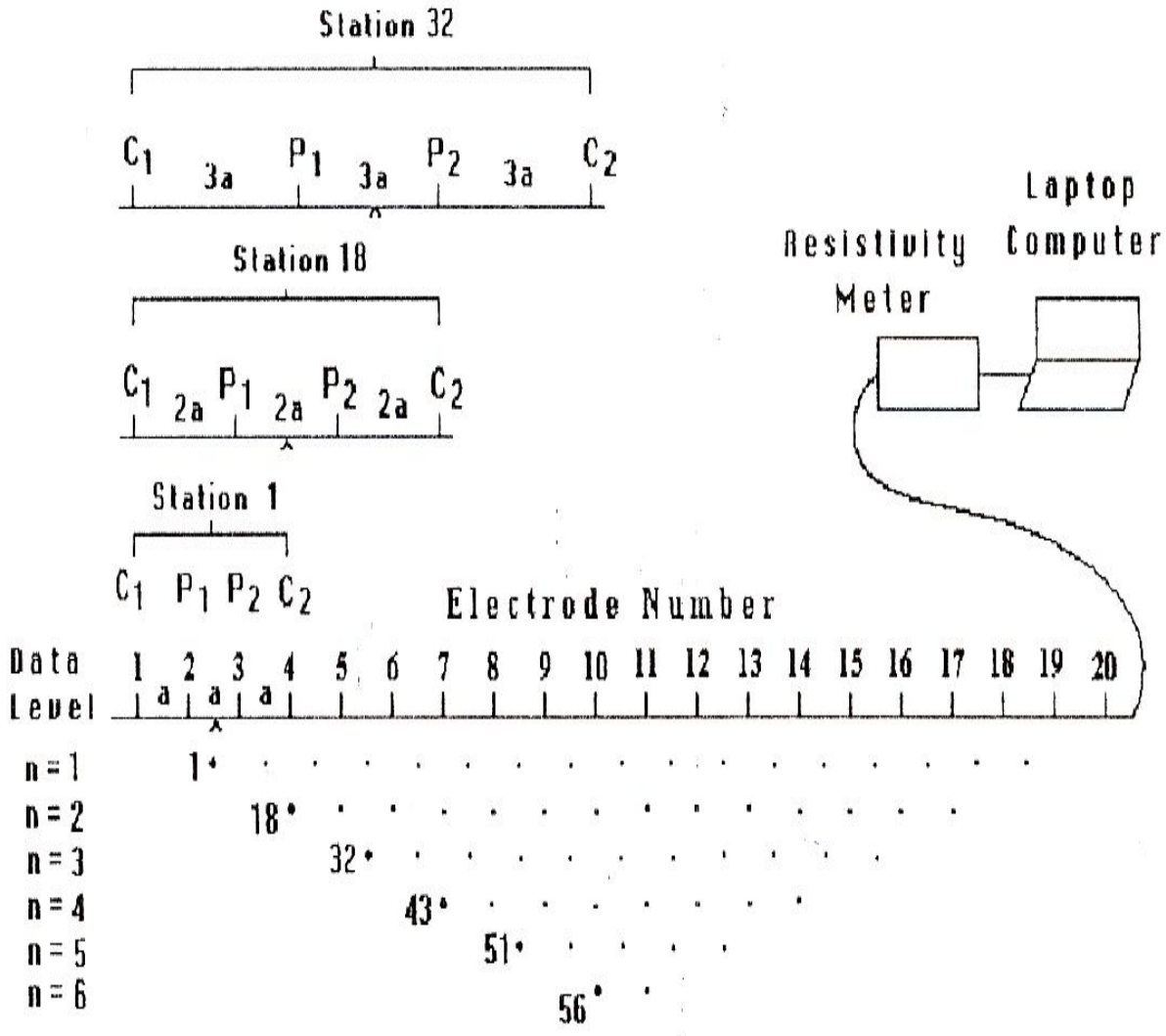


Figure 3.5 Measurement Procedures with Wenner Array

For the second measurement, electrodes 2, 4, 6 and 8 are used. This process is repeated down the line until electrodes 14, 16, 18 and 20 are used for the last measurement with spacing "2a". The same process is repeated for measurements with "3a", "4a", "5a" and "6a" spacing. To get the best results, the measurements in a field survey should be carried out in a systematic manner so that, as far as possible, all the possible measurements are made. This will affect the quality of the interpretation model obtained from the inversion of the apparent resistivity measurements (Dahlin and Loke 1998).

One technique used to extend horizontally the area covered by the survey, particularly for a system with a limited number of electrodes, is the roll-along method. After completing the sequence of measurements, the cable is moved past one end of the line by several unit electrode spacings. All the measurements which involve the electrodes on part of the cable which do not overlap the original end of the survey line are repeated.

CHAPTER FOUR

INTERPRETATION AND RESULTS

4.1 Introduction

As in all other geophysical methods the interpretation of data from electrical imaging involves expressing in geological terms the information given by the measured apparent resistivity data.

Electrical resistivity surveys are among the most difficult of all the geophysical methods to interpret quantitatively because of the complex theoretical basis of the technique (Keary and Brooks, 1996).

The resistivity method utilizes a potential field and consequently suffers from similar ambiguity problems to the gravitational and magnetic methods.

4.2 Interpretation Technique

The raw field data obtained for this work were processed using Res2Dinv (Loke and Barker 1996). To interpret the data from a 2-D imaging survey, a 2-D model for the subsurface which consists of a large number of rectangular blocks is usually used (Fig.4.1). A computer program is then used to determine the resistivity of the blocks so that the calculated apparent resistivity values agree with the measured values from the field survey. The computer program RES2DINV. EXE will automatically subdivide

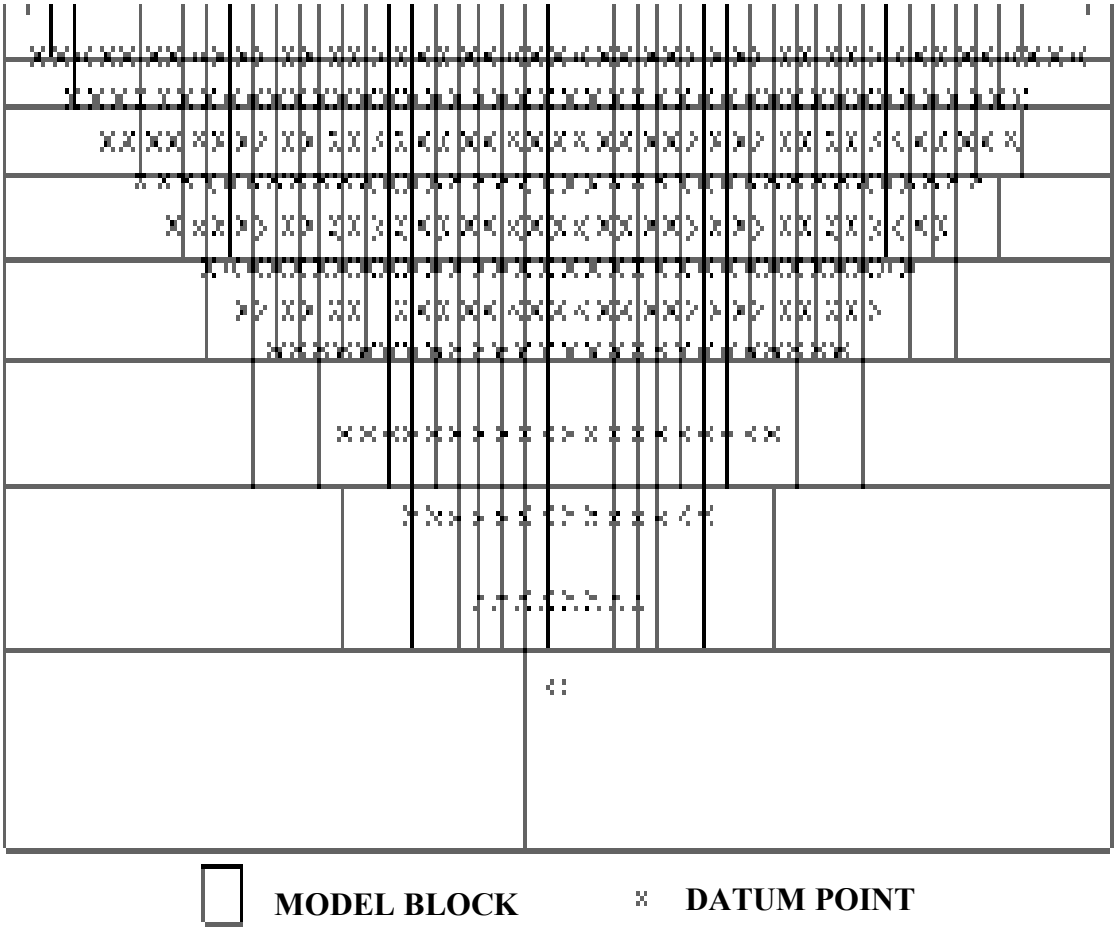


Figure 4.1 Arrangement of model blocks and apparent resistivity datum points

the subsurface into number of blocks and it then uses a least – squares inversion scheme to determine the appropriate resistivity value for each block. The location of the electrodes and apparent resistivity values must be entered into a text file which can be read by the RES2DINV program.

The RES2DINV program is designed to operate, as far as possible, in an automatic and robust manner with minimal input from the user. It has a set of default parameters which guides the inversion process. It uses a least – squares inversion to convert measured apparent resistivity values to true resistivity values and plots them in cross – section. The program creates a resistivity cross – section, calculates the apparent resistivities for that cross – section, and compares the calculated apparent resistivities to the measured apparent resistivities. The iteration continues until a combined smoothness constrained objective function is minimized.

The quality of the models produced depends on the data quality. To get a good model, the data must be of equally good quality. If the data is of poorer quality with unusually high or low apparent resistivity values, certain things can be done to improve upon the quality of the data. The first step is to look at the apparent resistivity Pseudosection. If there are spots with relatively low or high values, they are likely to be bad data points. With the RES2DINV program, data can be plotted in profile form that helps to highlight the bad datum points, and remove them from

the data set manually (fig 4.2). If the bad datum points are more widespread and random in nature, there are two program inversion

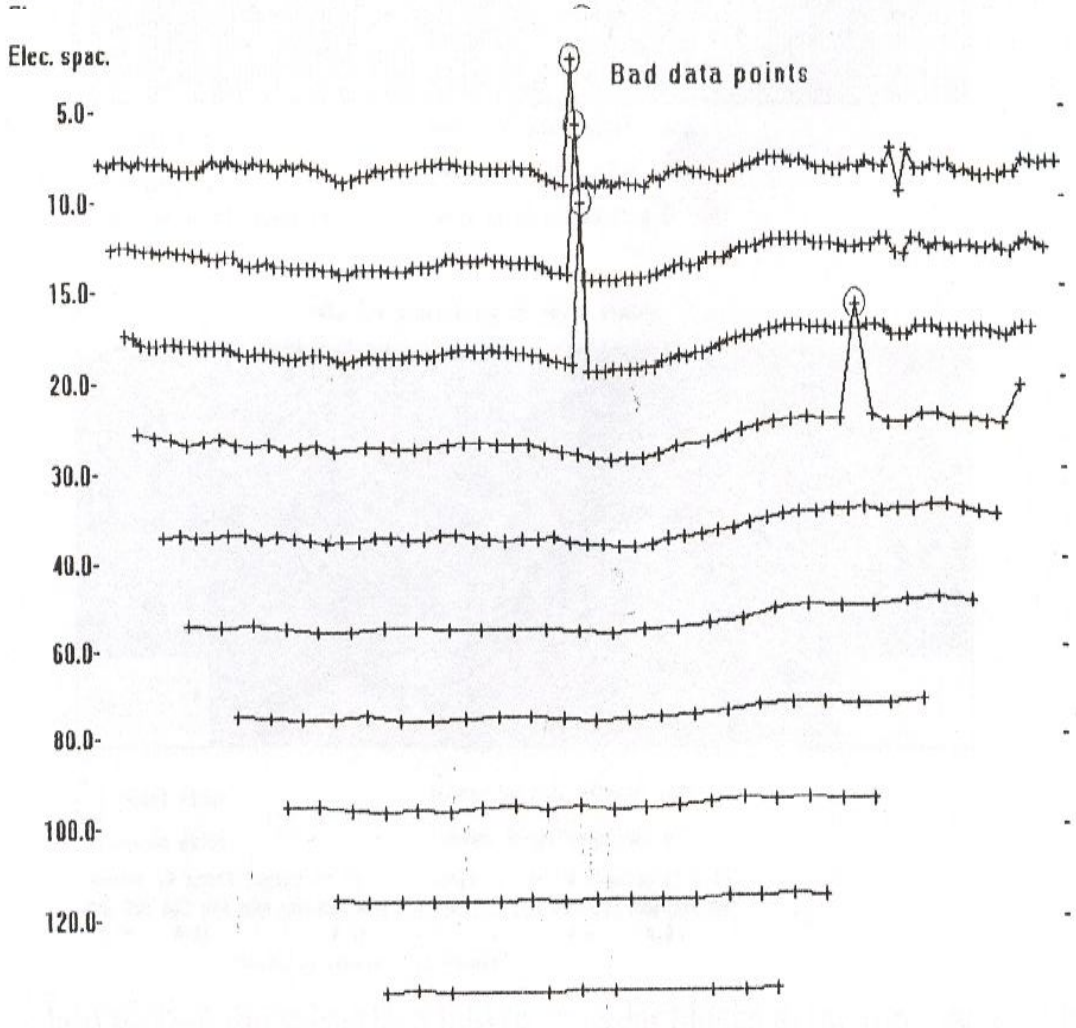


Figure 4.2 A Profile showing example of a data set with a few bad data points

parameters that can be modified. Firstly, the damping factor can be increased and the second setting is the robust data constrain option. These methods were adopted in improving on the quality of data obtained in this work.

4.3 Geological Control

A good knowledge of geology of an area is very important for any meaningful interpretation of any geophysical data collected from the area. In this work the borehole lithological log within the study area was used (Table 4.1).

Table 4.1 Lithology and Aquifers Borehole log (Groundwater Research Department National water Resources Institute, Kaduna).

Depth (m)		THICKNESS (m)	LITHOLOGY
FROM	TO		
0	15	15	Reddish brown laterite
9	21	6	Brownish sandy clay
21	42	21	Weathered basement
42	-	-	Fresh Crystalline Rock

4.4 The Inversion Method

All inversion methods essentially try to find model for the subsurface whose response agrees with the measured data. In the cell-based method used by the RES2DINV program, the model parameters are the

resistivity values of the model blocks, while the data is the measured apparent resistivity values. It is well known that for the same data set, there is a wide range of models whose calculated apparent resistivity values agree with the measured values to the same degree. Besides trying to minimize the difference between the measured and calculated apparent resistivity values, the inversion method also attempts to reduce other quantities that will produce certain desired characteristics in the resulting model. The additional constrains also help to stabilize the inversion process. The RES2DINV program uses an iterative method whereby starting from an initial model, the program tries to find an improved model whose calculated apparent resistivity values are closer to the measured values.

The inversion routine used by the program is based on the smoothness-constrained least-squares method (deGroot-Hedlin and Constable 1990, Sasaki 1992). The method is based on the following equation:

$$(J^T J + uF)\, d = J^T g - uFr \qquad (4.1)$$

Where F = a smoothing matrix.

J = the Jacobian matrix of partial derivatives.

r = a vector containing the logarithm of the model resistivity values.

u = the damping factor

d = model perturbation vector

g = the discrepancy vector.

The discrepancy vector, g, contains the difference between the calculated and measured apparent resistivity values. The magnitude of the vector is frequently given as a RMS (root-mean-squared) value. This is the quantity that the inversion method seeks to reduce in an attempt to find a better model after each iteration. The model perturbation vector, d, is the change in the model resistivity values calculated using the above equation which normally results in an "improved" model. The above equation tries to minimize a combination of two quantities, the difference between the calculated and measured apparent resistivity values as well as the roughness of the model resistivity values. The damping factor, u, controls the weight given to the model smoothness in the inversion process. The larger the damping factor, the smoother will be the model but the apparent resistivity RMS error will probably be larger.

The basic smoothness – constrained method can be modified in several ways that might give better results in some cases. The elements of the smoothing matrix, F, can be modified such that vertical or horizontal changes in the model resistivity values are emphasized in the resulting model.

4.5 The Production of Pseudosection

The first stage in the production of an electrical image is the construction of a Pseudosection (Baker 1989, Edwards 1977). It is a common method for qualitative presentation of resistivity data.

A Pseudosection is made by plotting the data points in a diagram, using the length axis for the distance along the surveying line and the depth axis for the electrode separations. The distance for the electrode configuration midpoint is thus plotted against the electrode separation for each measured data point.

The corresponding apparent resistivities for the plotted points are then used to contour the variation in apparent resistivity along the surveying line. The Pseudosection thus obtained reflects the variation of resistivity in the ground in a qualitative way. Figure 4.3 shows an example of a Wenner Pseudosection. Pseudosection is simply a 2D equivalent of the plotted field data points in a VES diagram.

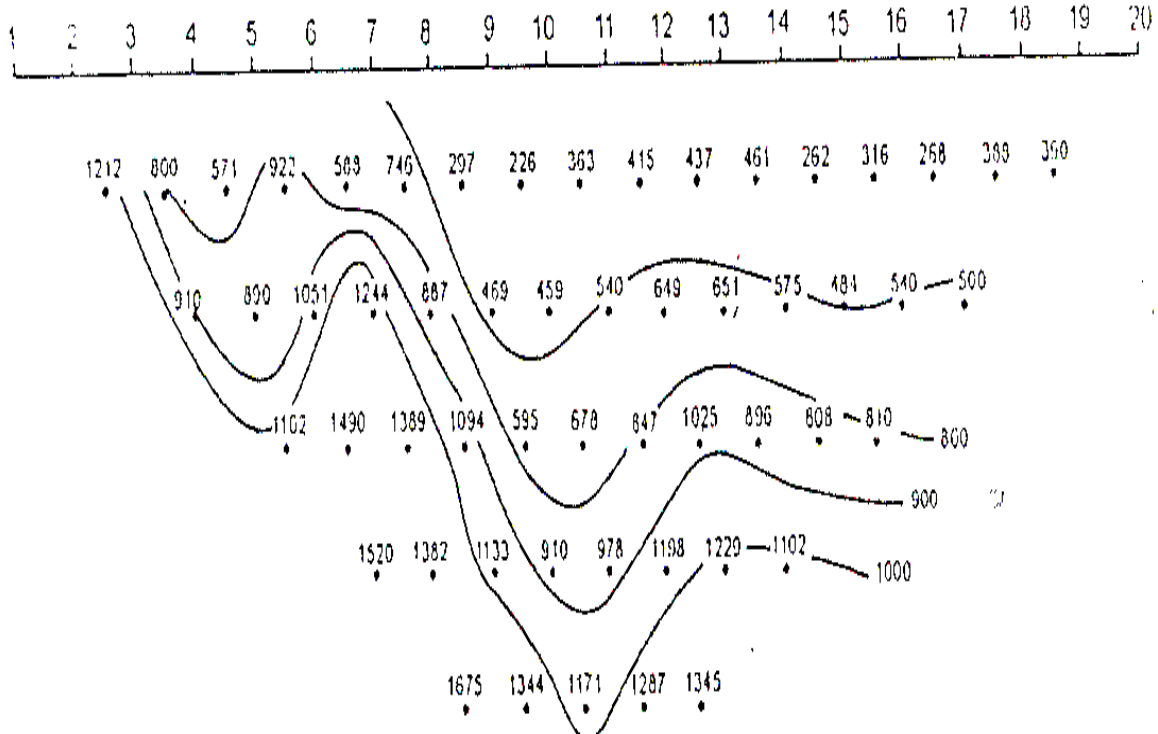


Figure 4.3 An example of a Wenner Pseudo - section

4.6 Electrical Images along the Profiles

A total number of five profiles were laid along the periphery of the dam and resistivity investigations were conducted along the five lines. The resulting measured apparent resistivity pseudosections which is obtained by plotting the observed apparent resistivity data against the pseudo-depth with colour in fill instead of line contours, the calculated apparent resistivity Pseudosection which is obtained by plotting the calculated apparent resistivity data against the pseudo-depth with colour infill instead of line contours also and the inverse model resistivity section which is obtained by performing a least-squares fitting between the observed values and the calculated values are shown.

4.6.1 Profile One

Figure 4.4 shows the measured apparent resistivity pseudosection, the calculated apparent resistivity pseudosection and the inverse model resistivity section of profile one. The inverse model resistivity section (fig. 4.4c) reveals three distinct layers, ranging from top soil which is reddish brown laterite to fractured basement. The near surface material is intercalation of sandy and lateritic clay with resistivity values ranging from about 26Ωm to about 75Ωm and thickness of about 15m. The materials

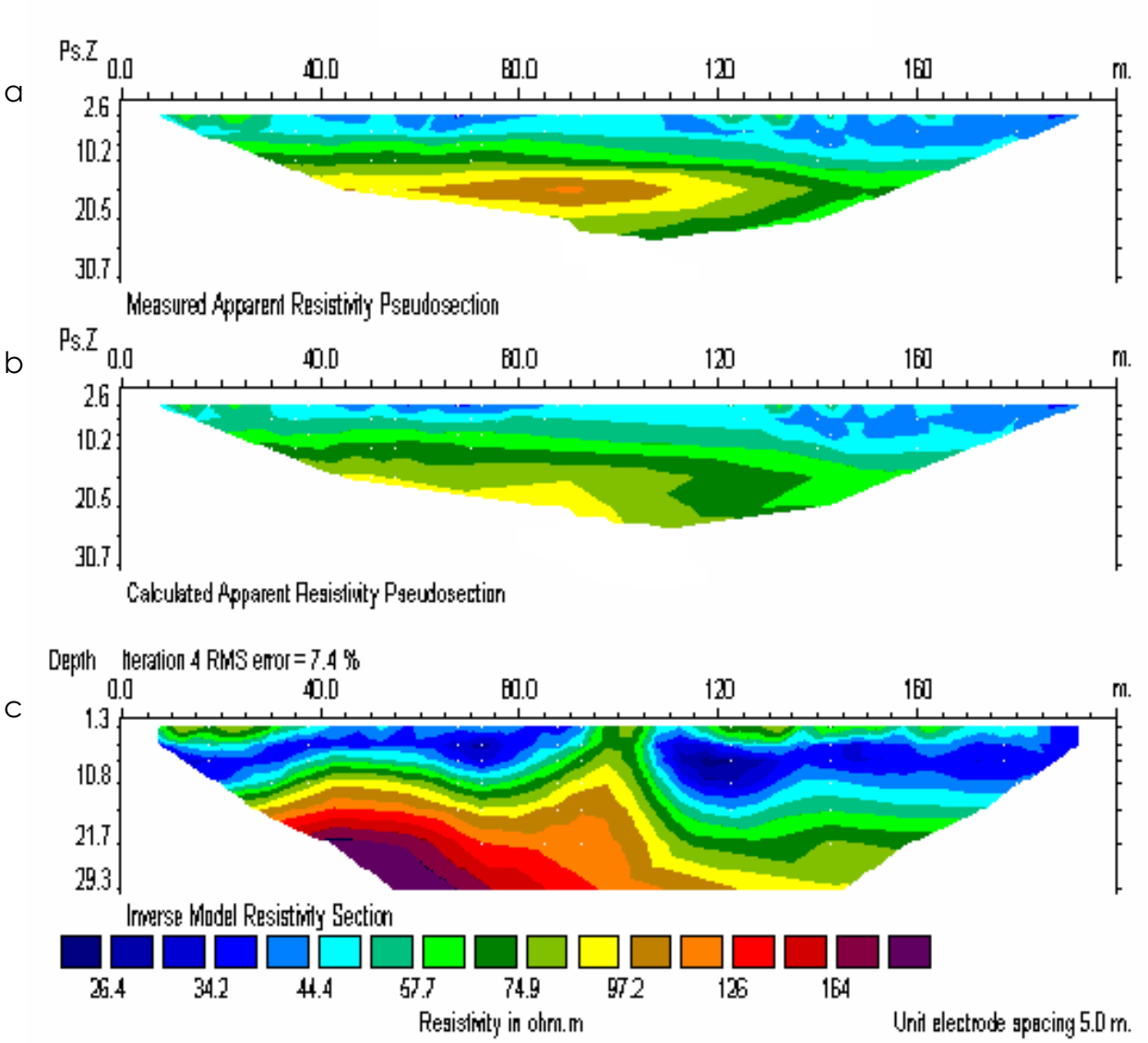


Figure 4.4 (a) Measured Apparent Resistivity Pseudosection. (b) Calculated Apparent Resistivity Pseudosection. (c)Inverse Model Resistivity Section for Profile One

extend to about 20m below the surface towards the end of the profile. The basement is highly fractured. This is observed in the low resistivity values (about 164Ωm) of the materials underlying the clay which is second distinct layer in the model.

The low resistivity values of the layers is a clear evidence that they are saturated with water, since the resistivity of rock decreases as the percent water saturation increases.

4.6.2 Profile Two

Figure 4.5 shows the measured apparent resistivity pseudosection, the calculated apparent resistivity pseudosection and inverse model resistivity section of profile two.

A careful look at the inverse model resistivity section of this profile (fig 4.5c) shows intercalation of sandy and lateritic clay as the top soils with the thickness of about 18m and resistivity values ranging from about 40Σ m to about to 130Σ m. This corresponds with the standard resistivity values of clay. Underlying these layers is the weathered basement from the depth of about 18m to about 29m with resistivity values ranging from about 130 Σ m to 213 Σ m. The low value of the resistivity is a clear indication that the basement is highly fractured.

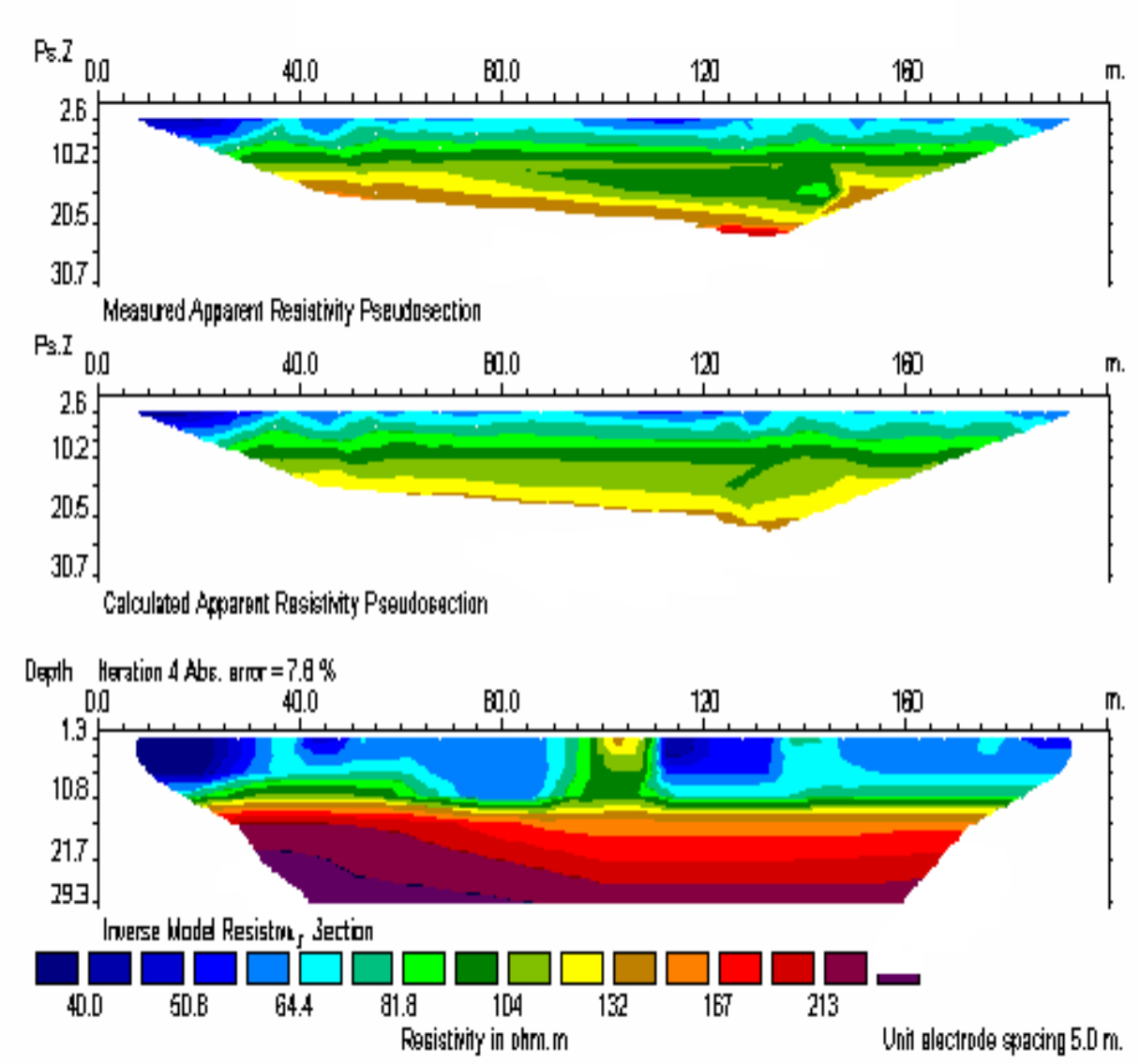


Figure 4.5(a) Measured Apparent Resistivity Pseudosection. (b) Calculated Apparent Resistivity Pseudosection. (c) Inverse Model Resistivity Section for Profile Two.

4.6.3 Profile Three

Figure 4.6 shows the measured apparent resistivity pseudosection, the calculated apparent resistivity pseudosection and the inverse model resistivity section of profile three. The inverse model section of the profile (fig. 4.6c) shows three layers.

The first layer which is a mixture of lateritic clay and sandy clay extends from the surface to a depth of about 16m with the resistivity values ranging from about 20Σm to about 60Σ m. These low resistivity values show that the materials in this layer are saturated with water. The intermediate layer which extends from about 16m to about 23m and even 25m below the surface in some part of the section with resistivity values ranging from about 63.0Ωm to about 78Ωm is believed to be clay material. The weathered basement which is severely fractured is the last layer on the section. It has a very low range of resistivity values (from about 79Ωm to about 100Ωm) which indicate high level of fracturing.

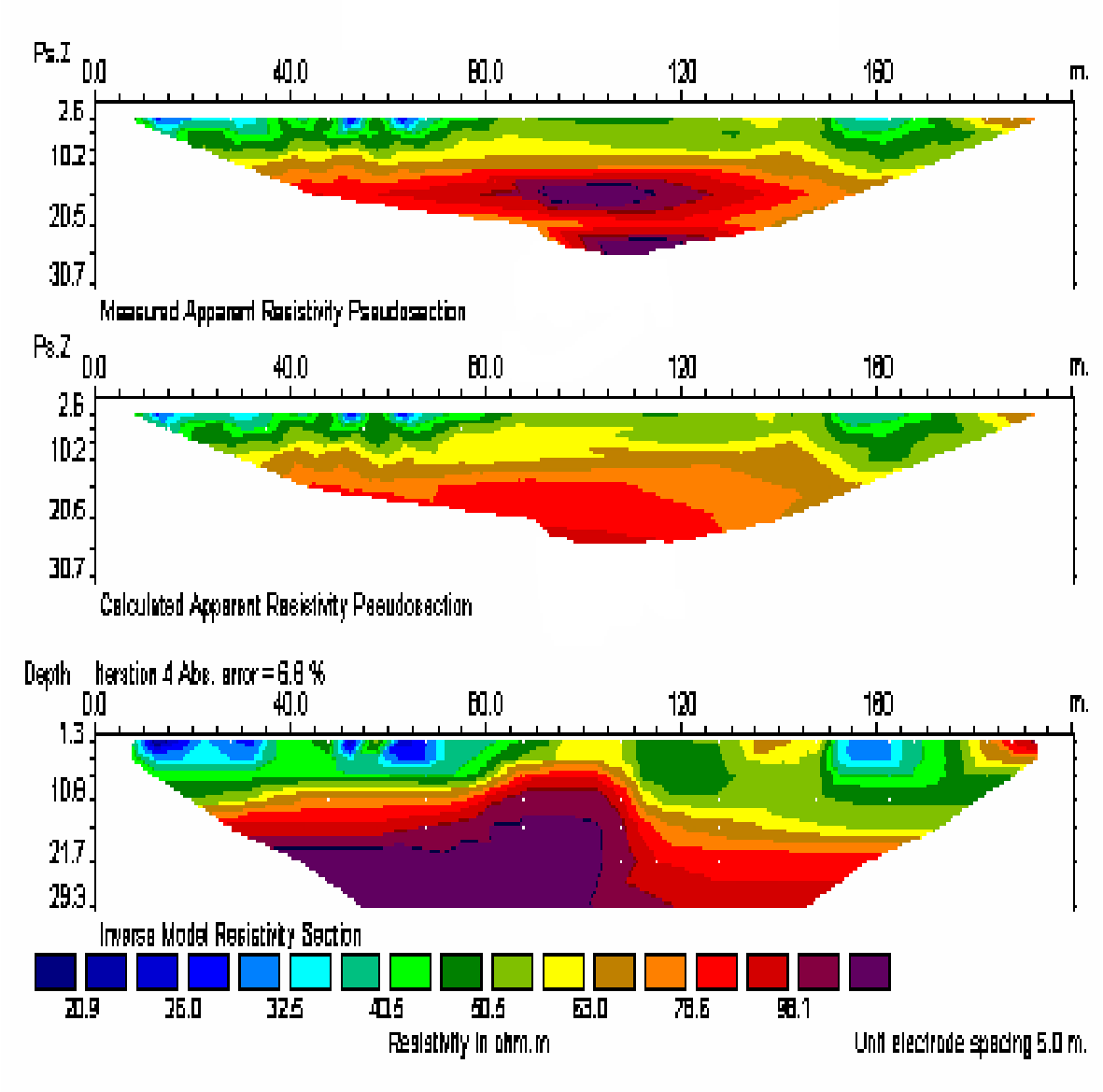


Figure 4.6(a) Measured Apparent Resistivity Pseudosection. (b) Calculated Apparent Resistivity Pseudosection. (c) Inverse Model Resistivity Section for Profile Three.

4.6.4 Profile Four

Figure 4.7 shows the measured apparent resistivity pseudosection, the calculated apparent resistivity pseudosection and the inverse model resistivity section of profile four. The inverse model resistivity section of profile (fig. 4.7c) shows low resistivity (19Σm - 50Σm) materials near the surface. The near – surface material is an intercalation of lateritic clay and sandy clay. The low value of the resistivity of these materials is a clear indication that the near surface materials are saturated with water and unconsolidated. Directly underlying these materials is the weathered basement with resistivity values ranging from about 50Σm and 68Σm. This low resistivity zone is considered to be a severely fractured basement.

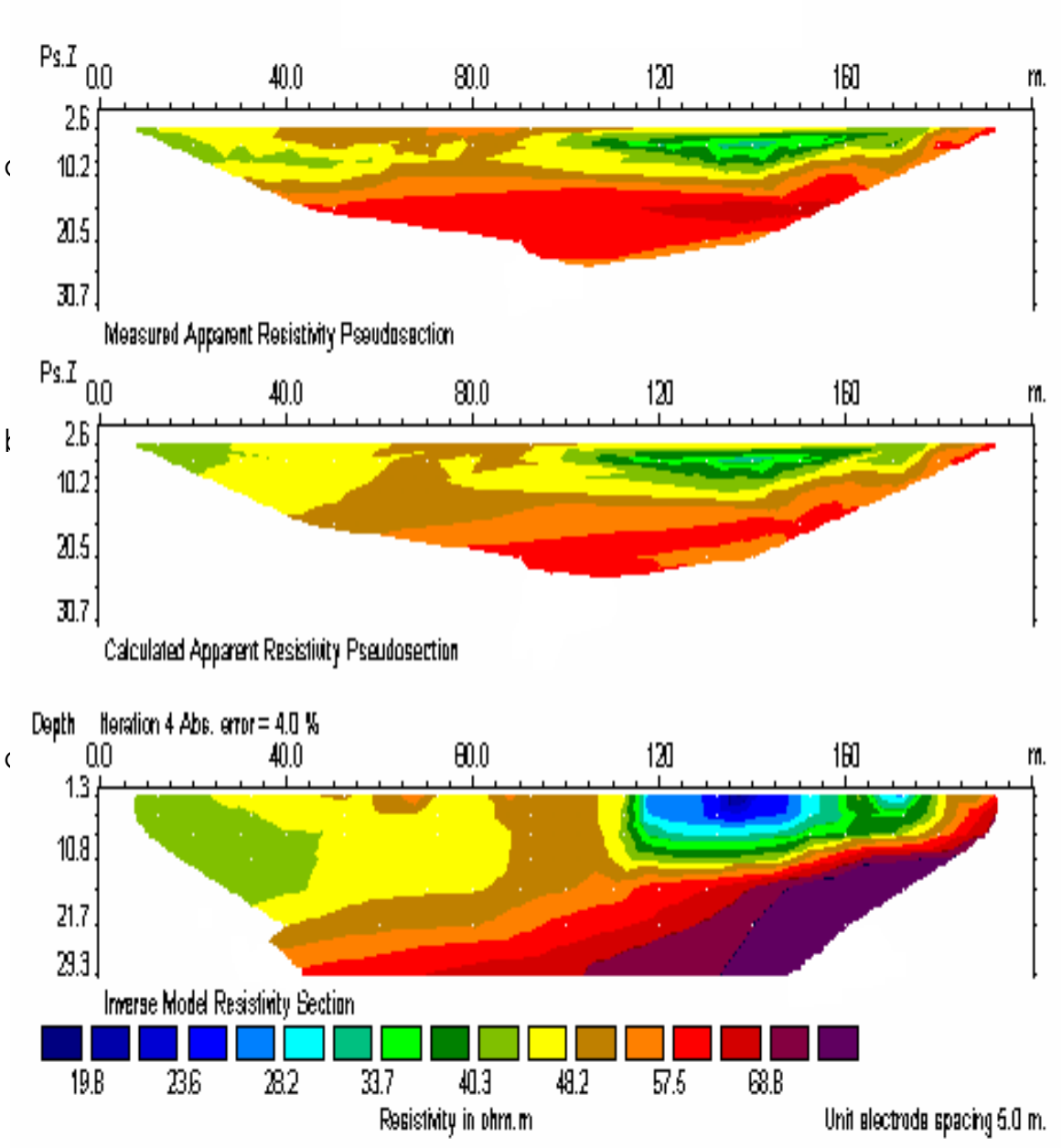


Figure 4.7(a) Measured apparent resistivity Pseudosection. (b) Calculated Apparent resistivity Pseudosection. (c) Inverse Model Resistivity Section for Profile Four.

4.6.5 Profile Five

Profile five was taken very close to the dam embankment. Figure 4.8 shows the measured apparent resistivity pseudosection, the calculated apparent resistivity pseudosection and the inverse model resistivity section of profile five. The inverse model resistivity section (fig. 4.8c) clearly reveals two layers with an anomaly of high resistivity value (about1461Σm) which is believed to be a boulder. The top soil with resistivity values between 28Σm and 88Σm is clay material while the bottom layer with resistivity values between 90Σm and 270Σm is weathered basement.

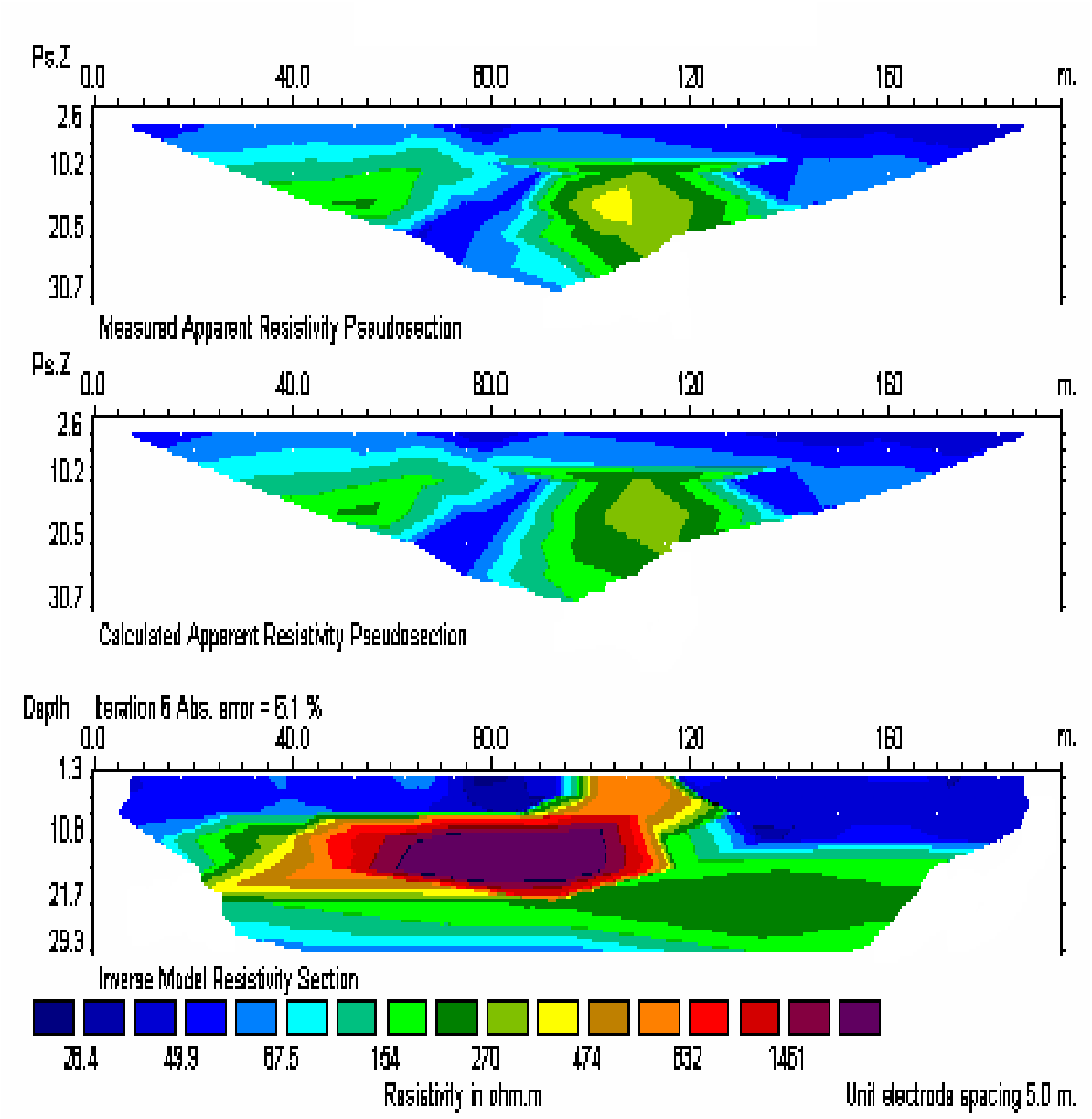


Figure 4.8(a) Measured Apparent Resistivity Pseudosection. (b) Calculated Apparent Resistivity Pseudosection. (c) Inverse Model Resistivity Section for Profile Five.

CHAPTER FIVE

CONCLUSION AND RECOMMENDATION

5.1 Conclusion

The major goal of this research was to study the subsurface structure of Bomo dam and investigate the possible cause of the seasonality of the dam. In connection with this goal the survey was carried out to determine the depth to the basement, the nature of the fracture system and the texture of the strata underlying the dam.

A total of five profiles were laid along the periphery of the dam and electrical imaging was carried out along the lines. Electrical images provide a more detailed view of subsurface structure than can be obtained using other geophysical techniques and may therefore lead to a better understanding of the fracturing system.

The inversion results of profile one reveal three distinct layers, lateritic clay, sandy clay and fractured basement. The low resistivity value of the layer is an indication that the materials are saturated with water. The electrical image also reveals that the basement is fractured. The electrical image of profile two shows intercalation of lateritic clay and sandy clay as near-surface materials with relatively thick weathered basement. The basement is fractured as clearly indicated by its low resistivity values (about 213 Ωm). The resistivity inversion result of profile three also reveals that the near-surface material is not uniform. It shows

that the weathered basement is highly fractured. This is evident from the low resistivity value (about 98 Ωm) of the basement. The depth to the weathered basement from the surface ranges from 15m at the beginning of the profile to about 20m towards the end of the profile. The resistivity inversion result of profile four also indicates that the near-surface is not uniform. The weathered basement is severely fractured as revealed by the low resistivity (about 68 Ωm) of the basement. The resistivity inversion result of profile five shows an anomaly with high resistivity value (about 1461 Ωm) which may likely be a boulder underlain by a weathered basement with relatively low resistivity value (about 270Ωm). This material with high resistivity value is likely to be part of the material used for the dam embankment.

The electrical images of the profiles show three distinct layers ranging from top soil, which is mainly intercalation of lateritic clay and sandy clay, to weathered basement. The low resistivity values of these layers indicate that the materials are saturated with water. None of the electrical images shows fresh basement. This indicates that the fresh basement is deeper than 29 m from the surface which agrees with the borehole lithological log within the study area. The average overburden thickness of the area is about 20m.

The results of this geophysical survey clearly show that the near-surface material is not consolidated. This suggests that excavation was

carried out during the dam construction. The top soil is made up of lateritic clay and sandy clay. The low resistivity values of the basement rock suggest that it is highly fractured.

It is therefore concluded from the results that the seasonality of the dam is partly due to both the fracturing of the weathered basement and the unconsolidated nature of the overburden.

5.2 Recommendation

It is recommended that geophysical survey should be carried out before any dam is constructed and it should also be employed as one of the dam monitoring tools.

Self potential (sp) surveys should be carried out in the survey area to further investigate the seapage condition of the dam. This should be followed up with 3D electrical imaging which gives a better picture of the subsurface Structure.

REFERENCES

ABEM Terrameter SAS 4000 / SAS 1000 instruction manual.

Acworth, R.I., 1987. The Development of Crystalline Basement Aquifers in a Tropical Environment: Quarterly Journal Engineering Geology. 20. 265 – 272.

Adamu, A.G.,1973. Basement Geology of Zaria – Samaru area, An Unpublished B.Sc. Project, Geology Department, Ahmadu Bello University, Zaria.

Akpoborie, I . A., 1972. Hydrogeological Control of Structures along Samaru Creek. Unpublished B.Sc. Thesis, Geology Department, Ahmadu Bello University, Zaria.

Ameloko, A.A., 2006. Two-Dimensional Electrical Imaging over the Western part of Kubanni Basin, Zaria, Nigeria. An Unpublished M.Sc. Thesis, Physics Department, Ahmadu Bello University, Zaria.

Archie, G.E., 1942. The Electrical Resistivity Log as an Aid in Determining some reservoir characteristics: Trans. Am Inst. Min. METAL. and Petr. Eng., V. 146 P. 54 - 62

Barker, R.D.,1989. Depth of Investigation of a Generalised Collinear 4 – Electrode Array. Geophysics, 54, 1031 – 1037.

Christensen, N.B. and Sorensen, K.I., 1994. Integrated use of Electromagnetic Methods for Hydrogeological Investigations. Proceedings of the Symposium on the Application of Geophysics to Engineering and Environmental Problems, March 1994, Boston, Massachusetts, 163 – 176.

Clark, N.J., 1960. Elements of petroleum reservoirs: SPE of AIME.

Dahlin, T.,1996. 2D resistivity surveying for environmental and Engineering applications. First Break 14 (7), 275 – 283.

Dahlin, T. and Loke, M. H., 1998. Resolution of 2D Wenner Resistivity Imaging as assessed by numerical modelling, journal of Applied Geophysics, 38, 237-249.

DeGroot – Hedlin, C. and Constable S., 1990. Occam's Inversion to Generate Smooth, Two – Dimensional Models from Magnetotelluric Data Geophysics, 55, 1613 – 1624.

Edwards, L.S.,1997. A Modified Pseudosection for Resistivity and Induced – Polarization. Geophysics, 42, 1020 – 1036.

Farouq, A. U., 2001. Geoelectric Investigation of the Groundwater Potential in the Institute for Agricultural Research Farm, Zaria; Unpublished M.Sc. Thesis, A.B.U., Zaria.

Grant, N.K.,1968. The late Precambrian to early Paleozoic Pan African Orogenic in Ghana Togo Dohomey, and Nigeria Geol. Soc, Am. Bull., vol. 80., p.p.45 – 56.

Griffiths, D. H. and Barker, R. D., 1993. Two – Dimensional Resistivity Imaging and Modelling in areas of Complex Geology. Journal of Applied Geophysics, 29, 211 – 226.

Habberjam, G.M.,1979. Apparent Resistivity and the use of Square Array Technique. Gebruder Borntraeger, Berlin.

Hore, P. N. 1970. Weather and climate Zaria and its Region. Ed. By M. J., Mortimore. Department of Geography, Occasional Paper No 4. A.B.U., Zaria. Pp 41 – 54.

Kearey, P. and Brooks, M. 1996. An Introduction to Geophysical Exploration. Geosciences Text. Blackwell Scientific Publications.

Keller, G. V. and Frischknecht, F. C., 1966. Electrical methods in geophysical prospecting pergamon Press.

Koefoed O. 1979. Geosounding Principles 1: Resistivity sounding Measurements. Elesvier Science Publishing Company, Amsterdam.

Loke, M. H. and Barker R. D. 1996. Rapid least – squares inversion of apparent resistivity pseudosections using a quasi – Newton method. Geophysical Prospecting, 44, 131 – 152.

McCurry, P. 1970. The Geology of the Zaria sheet 102 S.W. And it's Region. In: Mortimore, M.J. (Ed.). Department of Geography Occasional Paper No. 4 Ahmadu Bello University, Zaria.

Ososami, I. A. 1968. Assessment of the groundwater in the Kubani Valley. Unpublished M.Sc. Thesis A. B. U., Zaria.

Pazdirek, O. and Blaha, V.,1996 Examples of resistivity imaging using ME – 100 resistivity field acquisition system. EAGE 58th Conference and Technical Exhibition Extended abstracts, Amsterdam.

Sasaki, Y. 1992. Resolution of resistivity tomography inferred from numerical simulation. Geophysical Prospecting, 40, 453-464.

Slimark, S. and Djordjevic, N. 1987. Dam site engineering geophysics in Yugoslavia. First Break 5, (5), 161 – 171.

Trustwell, J.F. and Cope, R.N., 1963 . The Geology of parts of Niger and Zaria provinces, Northern Nigeria. GSN. Bulletin 29, 52p.

Wright, J.B. and McCurry, P., 1970. The geology of the Zaria sheet 102 SW. Zaria and its region Ed. By M.J. Mortimore. Department of Geography Occasional paper No.4 A.B.U, Zaria.